Aalborg Universitet

AALBORG UNIVERSITY
DENMARK

Structural Perspective on Fracture in Oxide Glasses

Januchta, Kacper

Publication date:
2019

Document Version
Publisher's PDF, also known as Version of record

Link to publication from Aalborg University

Citation for published version (APA):
Januchta, K. (2019). *Structural Perspective on Fracture in Oxide Glasses*. Aalborg Universitetsforlag.

General rights
Copyright and moral rights for the publications made accessible in the public portal are retained by the authors and/or other copyright owners and it is a condition of accessing publications that users recognise and abide by the legal requirements associated with these rights.

- Users may download and print one copy of any publication from the public portal for the purpose of private study or research.
- You may not further distribute the material or use it for any profit-making activity or commercial gain
- You may freely distribute the URL identifying the publication in the public portal -

Take down policy
If you believe that this document breaches copyright please contact us at vbn@aub.aau.dk providing details, and we will remove access to the work immediately and investigate your claim.

Downloaded from vbn.aau.dk on: April 25, 2024

STRUCTURAL PERSPECTIVE ON FRACTURE IN OXIDE GLASSES

BY
KACPER JANUCHTA

DISSERTATION SUBMITTED 2019

AALBORG UNIVERSITY
DENMARK

STRUCTURAL PERSPECTIVE ON FRACTURE IN OXIDE GLASSES

A PHD THESIS

by

Kacper Januchta

AALBORG UNIVERSITY
DENMARK

Dissertation submitted 2019

.

Dissertation submitted: 30-09-2019

PhD supervisor: Professor WSR Morten M. Smedskjær
Aalborg University

PhD committee: Associate Professor Jens Henrik Andreasen (chairman)
Aalborg University

Associate Professor Doris Möncke
Alfred University

Associate Professor Satoshi Yoshida
The University of Shiga Prefecture

PhD Series: Faculty of Engineering and Science, Aalborg University

Department: Department of Chemistry and Bioscience

ISSN (online): 2446-1636
ISBN (online): 978-87-7210-509-3

Published by:
Aalborg University Press
Langagervej 2
DK – 9220 Aalborg Ø
Phone: +45 99407140
aauf@forlag.aau.dk
forlag.aau.dk

© Copyright: Kacper Januchta

Printed in Denmark by Rosendahls, 2019

ENGLISH SUMMARY

One of the main drawback of glasses is their tendency to break if sufficient force is applied. This may compromise the usefulness of the glassy product, which poses an incentive for developing more damage resistant glass formulations. In order to facilitate a more efficient design of more damage-resistant glasses in the future, fundamental research concerning the brittle fracture mechanism and what governs it, is needed. In this thesis, the fracture behavior of glasses, specifically oxide glasses, are investigated from a chemical point of view. The aim of this work is to shed light on the correlation between chemical composition, the structural characteristics dictated by the composition, and the resulting mechanical properties.

In order to investigate the above mentioned correlations, each of the three aspects (chemistry, structure and properties) are accounted for. All oxide glasses presented in this work are synthesized by the traditional melt-quenching technique with a pre-determined chemical composition. Oxide glass systems studied herein include a) alkali and alkaline earth aluminoborates, b) sodium aluminoborosilicates, c) zinc lanthanum borates, and d) lanthanum aluminosilicate, aluminogermanate, and aluminoborate. The structural details of those glasses are studied mainly by Raman spectroscopy and nuclear magnetic resonance (NMR) spectroscopy. Finally, the mechanical behavior is investigated by indentation to probe the hardness and cracking tendency upon sharp contact loading, and by bending of single-edge-precracked-beam (SEPB) specimens to evaluate the fracture toughness. Different microscopy techniques are also used to support the indentation studies, as to shed light on the deformation mechanism of glasses subjected to sharp contact loading.

Based on the above mentioned investigations, the main findings are related to the role of the glassy network connectivity. More rigid, strongly polymerized glasses tend to resist deformation, e.g. during indentation, while more flexible, depolymerized glasses densify relatively easily. This allows the latter group to efficiently dissipate the supplied work, resulting in less driving force for crack initiation. However, the tendency to densify alone cannot be used as a reliable predictor of the resistance to indentation cracking, which appears to also be sensitive to strength of the bonds constituting the glassy network. Fracture toughness is sensitive to the network connectivity as well, with less cross-linked networks displaying less resistance to crack propagation through the possible avoidance of certain structural units. As a result, indentation cracking resistance and fracture toughness may in fact display opposite dependence on the network connectivity, which complicates the tuning of mechanical properties by adjustment of the chemical composition. Finally, this work found that atmospheric water may improve the indentation cracking resistance by a diffusion-swelling mechanism, which counteracts crack initiation and/or enhances stress dissipation.

DANSK RESUME

Én af de store ulemper ved glas af dets tendens til at knække hvis udsat for en tilstrækkelig kraft. Dette kan gøre et givent glasprodukt ubrugelig, hvilket skaber et incitament for at udvikle mere brudfaste glasformuleringer. For at muliggøre en mere effektiv design af mere brudfaster glasser i fremtiden, er der brug for grundforskning relateret til mekanismen for fraktur og hvad der styrer det. I denne afhandling vil frakturopførsel af glasser, særligt oxidglasser, blive undersøgt fra et kemisk synspunkt. Målet med dette studie er at belyse sammenhængen mellem den kemiske sammensætning, strukturelle karakteristika styret af sammensætningen og de resulterende mekaniske egenskaber.

For at undersøge den ovennævnte sammenhæng, er alle de tre aspekter (kemi, struktur og egenskaber) studeret. Alle oxidglasser præsenteret i dette studier blev syntetiseret vha. den traditionelle smelteafkølingsmetode, hvor glassernes sammensætning var forudbestemt. Oxidglasserne inkluderet heri omfatter a) alkali og jordalkali aluminoborater, b) natrium aluminoborosilikater, c) zink lanthan borater, og d) lanthan aluminosilikat, aluminogeramanat og aluminoborat. Strukturelle detaljer af disse glasser var hovedsagligt undersøgt via Raman spektroskopi og nuklear magnetisk resonans (NMR) spektroskopi. De mekaniske egenskaber blev studeret vha. indentering for at bestemme hårdhed og modstand mod revnedannalse ved skarp punkbelastning samt vha. bøjning af single-edge-precracked-beam (SEPB) emner for at bestemme brudsejhed. Diverse mikroskopi teknikker blev også brugt for at understøtte indenteringsstudier, nærmere bestemt for at belyse deformations-mekanismen af glasserne udsat for skarp punktbelastning.

Baseret på undersøgelserne nævnt ovenfor blev det klart, at de vigtigste resultater er relaterede til forbindelsesgraden af glasnetværket. Rigide, stærkt polymeriserede glasser lader til at modstå deformation, f.eks. under indentering, mens mere fleksible og depolymeriserede glasser densificerer relativt nemt. Dette muliggør de sidstnævnte glasser at relaksere det tilførte arbejde, hvilket resulterer i en mindre drivende kraft for revnedannelse. Tendensen til at densificere kan dog ikke stå alene som en pålidelig parameter til at forudse modstanden mod revnedannelse, hvilket også afhænger af styrken af de kemiske bindinger i glassets netværk. Brudsejheden er også sensitiv over for netværkets forbindelsesgrad, hvor mindre polymeriserede netværker udviser en mindre modstand mod revnevækst grundet mulig forbigåen af bestemte strukturelle enheder. Som følge heraf vil modstand mod revnedannelse og brudsejhed kunne udvise modsatrettede korrelationer med netværkets forbindelsesgrad, hvilket komplicerer styring af mekaniske egenskaber via justeringer af den kemiske sammensætning. Dette studie har også vist betydningen af luftfugtigheden, da atmosfærisk vand blev vist til at forbedre modstanden mod revnedannelse via en kvældning/diffusionsmekanisme, der modarbejder initiering af revner og/eller øger relaksationen af mekaniske spændinger.

ACKNOWLEDGEMENTS

I would like to express my gratitude to the VILLUM FONDEN (research grant no. 13253) for supporting my studies and travel.

I would like to thank my supervisor, Professor MSO Morten Mattrup Smedskjær for his investment in my work, his encouraging discussions, and for his always constructive criticism.

I would like to acknowledge all members of the VILLUM project group, Professor MSO Morten M. Smedskjær, Professor Yuanzheng Yue, Professor Marcel A. J. Somers, Malwina, Saber, Ang, Theany, Matteo, and Thomas, for their numerous advice with respect to my experiments and for creating an encouraging atmosphere.

I would like to thank all my collaborators, who made it possible to realize the goal of my studies through their excellent expertise and experience. I would like to highlight the roles of Dr. Randall E. Youngman for his help and guidance with respect to the tricky art of solid state NMR spectroscopy; Professor Mathieu Bauchy for sharing his knowledge on the importance of network topology; Associate Professor Lars R. Jensen for his ever-present helpfulness and assistance with Raman spectroscopy and mechanical testing; and Professor Tanguy Rouxel for his desire to make me understand every aspect of brittle solid mechanics.

I would like to thank the entire squad of the Mecanique et Verres group for their infinite hospitality during my external stay at Université de Rennes 1. Thank you for making my life in France such a memorable experience, Theany, Julien, Tanguy, Benjamin, Corentin, Gwénolé, Marion, Raveth, and Rodrigo.

I would like to thank my dear colleagues for upholding a fantastic working environment at the Section of Chemistry throughout the duration of my studies. I wish to highlight Rasmus, Mouritz, Laura, René, Saurabh, Jonas, Chao, Tobias, Martin, Nerea, Kasia, Mikkel, Søren, Søren, Søren, Rasmus, Johan, Ang, Pengfei, Sheng, Theany, and of course Anne-Sophie. A special thank you goes to Malwina for her true companionship throughout the three years of our parallel studies. My dearest apologies to those colleagues, who have been unmeaningfully overseen.

I would like to thank all members of my family, both the blood-related ones and the ones I married into, for their unconditional support and faith in my abilities.

Finally, the biggest thank you goes to my dear wife, Linea, mainly for her patience and understanding throughout this period, but also for her great spiritual support and even scientific guidance. It has been a much easier journey with your encouragement!

TABLE OF CONTENTS

CHAPTER 1. INTRODUCTION

1.1. MOTIVATION

We, humans, have the desire to solve any challenges we are facing in a faster, easier, or more clever way. Whether it is something significant such as transportation to the other side of the world, or something more ordinary like washing the dishes, we are finding ways to simplify our life and to produce a more efficient society. This demand has fueled the industrial development in the past and continues to do so, resulting in the discovery of new technological advancements on a daily basis.

Within the enormous scope of the term ‘technological advancements’ used above, the discovery and functionalization of glass has in fact played an essential role. Indeed, glasses surround us. As you are reading this introduction, you can probably find yourself being protected from wind and rain by a window, enjoying a refreshing beverage stored in a glassy container, and perhaps struggling a little less when browsing through the letters thanks to the pair of reading glasses supported by your nose and ears. These are just the obvious applications. Others include the use of glass fiber in wind turbine blades and fiber-optic cables, supplying your computer with power and internet, respectively. Or maybe, you are reading this on a smart-phone equipped with a glassy screen, which you may or may not have dropped on the floor yet. In case of the latter, there is a good chance that the brittle glass is broken, without the hope of restoring itself, which is a good example of why research in glass science is so important.

Despite the fact that the technique of producing glass from molten minerals was mastered already by ancient civilizations, there has been surprisingly little improvement with respect to overcoming the brittle behavior, which seems intrinsic to the glassy state. However, the industrial development saw glasses utilized in new applications creating an incentive for research within glass technology. At the same time, advances in science such as development of spectroscopy techniques gave researchers a great opportunity to shed light on the physics of the glassy state. Today, we are able to understand why the chemical composition, the thermal history, and the applied post-treatment method, have an effect on the properties of the glass. Nevertheless, we continue to struggle when we want to design more damage resistant glass formulations. The commercially available glass products become stronger and stronger for each generation, but their development is largely based on a trial-and-error approach. A better in-depth understanding of what controls the brittle fracture in glasses is necessary to accelerate the improvement of their mechanical properties to comply with the demands of our society.

1.2. SCOPE AND OBJECTIVES

The overall goal of the work summarized in this thesis has been to enhance the current state of understanding of brittle fracture in glass. More specifically, attention is turned towards the correlation between the chemical composition and the deformation and cracking behavior of glasses, while the effects of various post-treatment methods on the properties of glasses are outside the scope of this thesis. Furthermore, only studies on non-metallic inorganic glass systems, especially aluminoborates and aluminoborosilicates, are described herein. In other words, the thesis concentrates on the properties of pristine oxide glasses, and investigates how the chemical composition can be tuned to achieve more favorable mechanical properties. In summary, the thesis attempts to shed light on the following aspects:

- The impact of glass structure on the indentation deformation mechanism.
- The impact of chemical composition on the resistance to crack initiation.
- The impact of chemical composition on fracture toughness.
- The link between deformation mechanism and crack initiation.
- The correlation between resistance to crack initiation and fracture toughness.
- The influence of atmospheric conditions on crack initiation.

The purpose of this thesis is thus to deliver an overview of the most central conclusions drawn from the experiments carried out by the author. In order to capture the interest of as broad an audience as possible, the thesis starts by providing the reader with fundamental theory concerning brittle fracture mechanics (Chapter 2), as well as oxide glass structure (Chapter 3). Tools and techniques used by the author are highlighted in Chapters 2 and 3 as well to facilitate the ease of understanding the results described later on. The results connected to the link between glass structure and deformation mechanism are summarized throughout Chapter 4, while results connected to fracture-related properties are gathered in Chapter 5. In Chapters 4 and 5, the results are not listed chronologically, but rather arranged in a way that enables logic transitions between different aspects of the work. Finally, the main findings are summarized and discussed in Chapter 6.

1.3. THESIS CONTENT

The thesis is written as an extended summary of the findings reported in the peer-reviewed scientific papers published throughout the duration of the project, including one submitted manuscript that awaits publication. The papers listed below are cited by their roman numerals throughout the thesis.

I. **K. Januchta**, R.E. Youngman, A. Goel, M. Bauchy, S.L. Logunov, S.J. Rzoska, M. Bockowski, L.R. Jensen, and M.M. Smedskjaer, “Discovery of ultra-crack-resistant oxide glasses with adaptive networks”, *Chemistry of Materials*, **29** (2017) 5865-5876

II. **K. Januchta**, M. Bauchy, R.E. Youngman, S.J. Rzoska, M. Bockowski, and M.M. Smedskjaer, "Modifier field strength effects on densification behavior and mechanical properties of alkali aluminoborate glasses", *Physical Review Materials*, **1** (2017) 063603

III. K.F. Frederiksen, **K. Januchta**, N. Mascaraque, R.E. Youngman, M. Bauchy, S.J. Rzoska, M. Bockowski, and M.M. Smedskjaer, "Structural compromise between high hardness and crack resistance in aluminoborate glasses", *The Journal of Physical Chemistry B*, **122** (2018) 6287-6295

IV. **K. Januchta**, R. Sun, L. Huang, M. Bockowski, S.J. Rzoska, L.R. Jensen, and M.M. Smedskjaer, "Deformation and cracking behavior of La_2O_3-doped oxide glasses with high Poisson's ratio", *Journal of Non-Crystalline Solids*, **494** (2018) 86-93

V. **K. Januchta** and M.M. Smedskjaer, "Indentation deformation in oxide glasses: Quantification, structural changes, and relation to cracking," *Journal of Non-Crystalline Solids X*, **1** (2019) 100007

VI. **K. Januchta**, R.E. Youngman, L.R. Jensen, and M.M. Smedskjaer, "Mechanical property optimization of a zinc borate glass by lanthanum doping", *Journal of Non-Crystalline Solids*, **520** (2019) 119461

VII. **K. Januchta**, T. To, M. Bødker, T. Rouxel, and M.M. Smedskjaer, "Elasticity, hardness, and fracture toughness of sodium aluminoborosilicate glasses", *Journal of American Ceramic Society*, **102** (2019) 4520-4537

VIII. **K. Januchta**, M. Stepniewska, L.R. Jensen, Y. Zhang, M.A.J. Somers, M. Bauchy, Y. Yue, and M.M. Smedskjaer, "Breaking the limit of micro-ductility in oxide glasses", *Advanced Science*, (2019) 1901281

IX. **K. Januchta**, P. Liu, S.R. Hansen, T. To, and M.M. Smedskjaer, "Indentation cracking and deformation mechanism of sodium aluminoborosilicate glasses", manuscript submitted to *Journal of American Ceramic Society*

CHAPTER 2. FUNDAMENTALS OF BRITTLE FRACTURE

When a stone hits the windscreen of a car in motion, the glass surface is likely to suffer permanent damage, usually appearing as a relatively small chip. Over time, this may develop into a growing crack, compromising the integrity of the windscreen. This is a phenomenon known to most, but the underlying physics of the process may need additional explanation from a layman's point of view. In this chapter, the reader will be introduced to certain aspects of fracture mechanics, which are relevant for understanding the fundamentals of brittle fracture occurring in oxide glasses.

2.1. INDENTATION DEFORMATION MECHANISM

In a real life environment, glass surfaces are constantly in contact with hard, sharp objects. The object can have different material properties, shape, and velocity of impact, which complicates the analysis of the damage event. In order to enable efficient research within the field of brittle fracture induced by sharp contact loading in glasses, one can mimic the real life situation by a controlled test in the laboratory. An example of such a test is indentation (Figure 2-1), wherein the loading material, the geometry of the object, and the loading conditions are known to the operator. A thorough literature review concerning indentation of glasses is given in Paper V, but some central aspects of this technique are summarized in the following.

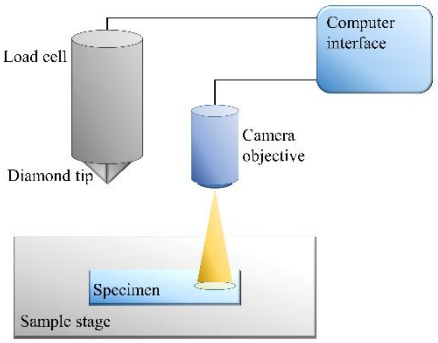

Figure 2-1 Schematic representation of an indentation setup. The glass specimen is supported on top of a sample stage. In order to induce damage, the diamond tip is lowered into the surface of the glass, and the applied load is measured via a load cell. The load can be controlled via a computer interface. A camera objective, also connected to a computer, can then be used to record an image of the site.

For oxide glasses, the preferred configuration of testing is the use of a four-faced diamond pyramid, which penetrates the glass surface with a peak load of a few mN to a few N in the normal direction. Diamond is used, as it is significantly more stiff then any oxide glass and can therefore be considered rigid. The commonly used four-faced pyramidal geometry (called Vickers) is adequate for the induction of permanent residual imprints in the glass surface, which can easily be analyzed *post mortem*. Given the brittle nature and relatively high hardness of oxide glasses, the size of the Vickers imprints is usually restricted to the µm range, inducing the need for a microscope evaluation.

During loading with a Vickers pyramidal indenter, the material initially responds elastically. This is due to the indenter tip not being perfectly sharp [1]. With increasing load however, plasticity is induced as well. The plastic response of an oxide glass consists of densification and shear flow [2, 3]. The different types of deformation have been schematically illustrated in Figure 2-2. Densification in glasses occurs as a result of structural rearrangements on the atomic scale leading to a more efficient packing of the atoms, while shear flow is essentially a displacement of atoms occurring through continuous breakage and reformation of bonds.

Figure 2-2 Schematic representation of the deformation mechanism undergoing during indentation. The pristine glass subjected to loading exhibits plastic deformation resulting in a hemispherical area of densified material (dark blue). Upon unloading, part of the material springs back due to elastic recovery. Annealing of the glass results in relaxation of the densified part, resulting in a smaller indent cavity surrounded by a ridge of recovered material.

The volumetric distribution between these two mechanisms depends on the chemical composition of the glass [4]. Ultimately, this difference also has a significance for the characteristic cracking pattern of the given glass [5]. Upon unloading of the indenter, the elastically strained material attempts to recover, but is hindered by the permanently deformed plastic zone. This leads to the storage of residual stresses, which may initiate formation of cracks if they are tensile and of sufficient magnitude [6, 7].

As it is of interest to know, or at least estimate, the magnitude of residual stresses stored in the glass *post*-indentation, a technique to quantify the extent of densification has been suggested [4]. The focus lies on densification, as it has been claimed to be an efficient mechanism to dissipate the work supplied by the indenter during loading [8]. The characteristic of the densified material and the nature of the displacement mechanism differs from shear flow. This can be used to induce recovery of

densification at sub-T_g temperatures, while such temperatures are not sufficient to activate viscous flow, leading to sole recovery of the densified volume. By recording a topographic image of the indent cavity site using a tool, such as atomic force microscopy (AFM), before and after the thermal treatment, it is possible to evaluate the difference in shape of the cavity. This change in shape is directly relatable to the extent of recovered volume, or in other words, the volume displaced by densification. In detail, the relative extent of densification can be expressed as volume recovery ratio (V_R), calculated as:

$$V_R = \frac{(V_i^- - V_a^-) + (V_a^+ - V_i^+)}{V_i^-}, \tag{2.1}$$

where V is the volume of the indent site, the superscripts – and + relate to the volume below and above the surface of the glass, while the subscripts i and a relate to the initial state and annealed state of the indent. An example of topographical maps acquired for the initial and the annealed states of an indent site, respectively, are given in Figure 2-3. As such, the use of AFM itself is not crucial, as other techniques with the ability to produce topographic representations of the indentation site may be employed instead, e.g. laser microscopy [9].

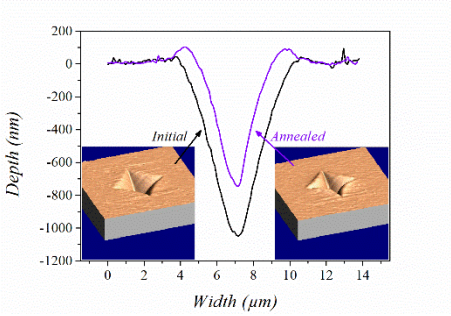

Figure 2-3 Topographical representations of an initial (left) and annealed (right) states of an indent site along with cross sections through the center of the indents. Data acquired from atomic force microscopy measurements on a lithium aluminoborate glass. Figure adapted from Paper I.

AFM measurements are time- and resource-consuming, which hampers efficient collection of densification data for oxide glasses. Meanwhile, similar information can be extracted from optical microscopy. The shape of the indent changes upon thermal treatment, which can be readily observed from optical microscopy, as illustrated in Figure 2-4.

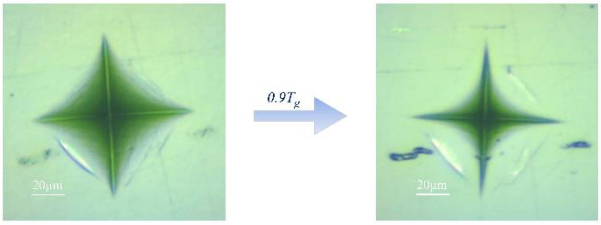

Figure 2-4 Optical microscopy images of an indent site before (left) and after (right) a sub-T_g annealing treatment. The images clearly illustrate that the length of the sides (distance from one edge to opposite edge across the indent center) recovers due to annealing. The length of the diagonals (distance from corner to corner across the indent center) do not recover significantly. The indent was produced in a sodium aluminoborate glass.

Especially the shrinkage in the side length is significant, while the recovery of the diagonal length is close to zero. In this work, an analogous parameter to V_R has been suggested, namely the side length recovery (L_{SR}), which can be computed from indent side length recovery before and after annealing:

$$L_{SR} = \frac{L_{S,i} - L_{S,a}}{L_{S,i}}, \tag{2.2}$$

where L_S is the indent side length (edge to edge), and subscripts *i* and *a* refer to initial and annealed states, respectively. In general, the L_{SR} parameter scales well with V_R for a wide range of oxide glass systems (Paper IX), as shown in Figure 2-5. This paves the way towards more efficient quantitative studies of indentation deformation mechanism in the future.

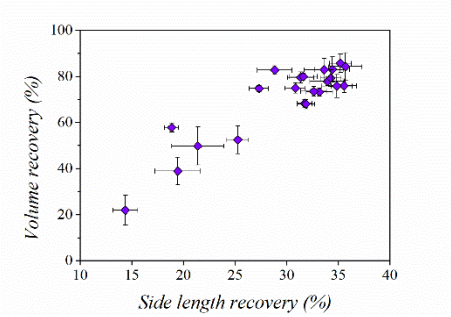

Figure 2-5 Positive correlation between volume recovery ratio and indent side length recovery ratio for a range of different oxide glass systems. Data points correspond to amorphous silica, aluminoborate, silicate, aluminosilicate, and aluminogermanate glasses (see details in Paper IX). Figure adapted from Paper IX.

2.2. INDENTATION CRACKING

The characteristic of cracking in oxide glasses depend on the magnitude of residual tensile stresses stored around the indented area. However, it is challenging to describe the indentation stress field. Nevertheless, several researchers have suggested analytical models that attempt to capture the contact event, with the "expanding cavity" model being the most widely accepted [10]. A frequently applied solution to the indentation problem is the elastic stress field proposed by Yoffe [11], which deals with an axis-symmetric loading of an infinite half-space with a conical indenter tip. This model presents the distribution of elastic stresses outside the plastic zone. The elastic stresses operating in Yoffe's field define the potential for opening of cracks in a given position and direction. The crack systems found in oxide glasses are median, half-penny, radial, lateral and cone [5], as shown in Figure 2-6.

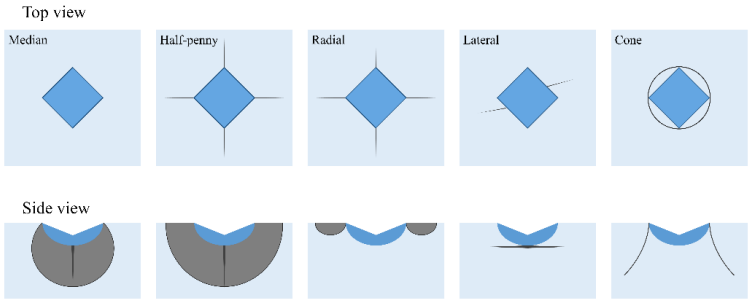

Figure 2-6 Schematic representation of characteristic crack patterns commonly found in oxide glasses. Top and side perspectives are shown to illustrate the differences in in the cracking mechanisms.

The magnitude of stress for a given crack system depends on the loading configuration, the material properties, and the distance from the point of contact. These stresses can be calculated in spherical coordinates (r, θ, ϕ) as:

$$\sigma_{rr}(r,\theta) = \frac{P}{2\pi r^2}[1 - 2\nu - 2(2-\nu)\cos\theta] + \frac{B}{r^3}4[(5-\nu)\cos^2\theta - 2 + \nu], \quad (2.3)$$

$$\sigma_{\theta\theta}(r,\theta) = \frac{P}{2\pi r^2}\frac{(1-2\nu)\cos^2\theta}{1+\cos\theta} - \frac{B}{r^3}2(1-2\nu)\cos^2\theta, \quad (2.4)$$

$$\sigma_{\phi\phi}(r,\theta) = \frac{P}{2\pi r^2}(1-2\nu)\left[\cos\theta - \frac{1}{1+\cos\theta}\right] + \frac{B}{r^3}2(1-2\nu)(2-3\cos^2\theta), \quad (2.5)$$

$$\sigma_{r\theta}(r,\theta) = \frac{P}{2\pi r^2}\frac{(1-2\nu)\sin\theta\cos\theta}{1+\cos\theta} + \frac{B}{r^3}4(1+\nu)\sin\theta\cos\theta, \quad (2.6)$$

$$\sigma_{r\phi}(r,\theta) = \sigma_{\theta\phi}(r,\theta) = 0, \quad (2.7)$$

where P is the normal load of the indenter, v is the Poisson's ratio of the glass, and B is the Blister field strength. For all stresses driving indentation cracking, it is true that their magnitude decreases with increasing distance from the point of contact. Hence, the most probable point of crack initiation, i.e., the point with the highest tensile stress, is just outside the plastic zone.

There is currently no consensus in the literature with respect to how to quantify the strength of the Blister stress field. However, the literature agrees that the Blister field strength is a function of the material properties, and that it correlates inversely with the extent of densification [5]. Having an estimate of the value of B and knowledge of the material properties for a given glass makes it possible to predict which stresses are tensile, and hence which type of cracking is expected. As such, it is believed that glasses with low B are more damage-resistant than high-B glasses, as a larger fraction of the work supplied by the indenter dissipates by means of densification [12]. Furthermore, it appears that low v-values tend to densify easily, and exhibit cone cracking, while glasses with higher v-values also undergo extensive shearing during indentation, and display median and/or radial cracking behavior (Figure 2-6). The former glasses are often called "anomalous", while the latter are called "normal" [7]. Experimental proof of the differences in the deformation and cracking behavior for normal and anomalous glasses was presented by Arora et al. [7], see Figure 2-7.

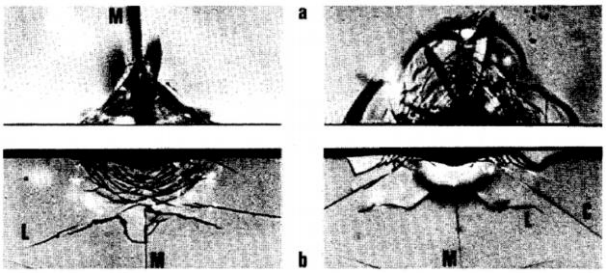

Figure 2-7 Top view (top) and cross-section view (bottom) of the damage induced by Vickers indentation in window glass (left) and amorphous silica (right). The images clearly illustrate the differences in cracking behavior between normal and anomalous glasses. Figure reprinted from Arora et al. [7] *with permission of Elsevier.*

The model suggested by Yoffe (valid for a conical indenter) does not reproduce the Vickers indentation stress field accurately due to the difference in indenter geometry. Nevertheless, the general trends in pyramidal and conical indenter tips are the same, making the model a reasonable approximation of a sharp contact event [1]. In fact, the characteristic cracking pattern of a given oxide glass can be predicted based on its material properties using Yoffe's model with a reasonable accuracy [12]. However, prediction of the critical load for crack initiation remains challenging. The current state-of-the-art regarding the quantification of the critical load for crack initiation involves systematic indentation testing. The most frequently used approach is that suggested by Wada [13], where the probability of corner cracks (radial or median half-

penny) following Vickers indentation is determined for systematically increasing loads. The resistance to indentation crack initiation, *CR*, is defined as the load resulting in 50 % probability of corner crack initiation according to Wada methodology [13]. An example of determination of *CR* for an arbitrary glass composition is given in Figure 2-8.

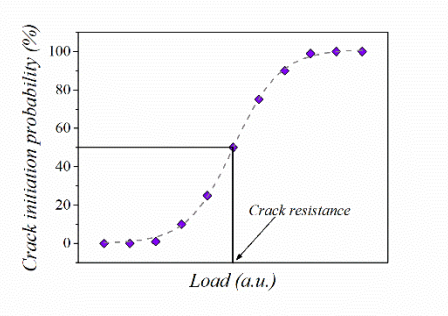

Figure 2-8 Schematic representation of how to compute crack resistance for a given glass. The crack initiation probability is calculated for each of the applied loads. A sigmoidal function is then fitted to the data. The load corresponding to 50 % crack initiation probability is defined as crack resistance.

2.3. FRACTURE MECHANICS

As described in previous section, surface cracks in glasses initiate upon contact with sharp objects. Once the cracks are present in a glassy specimen, they are potentially subject to growth if tension is applied to the specimen. In brittle materials, the presence of cracks is detrimental to their strength, as any tensile stress applied in the direction of crack opening actually amplifies at the crack tip [14]. Hence, relatively little force is required to induce fracture in a cracked specimen compared to a pristine one. As a result, the strength of brittle materials is always significantly lower than their theoretical strength, which can be calculated based on the interatomic bond strength [15]. On the other hand, decreasing the size of the specimen leads to an increase in the apparent strength approaching the theoretical one, e.g. glass fibers have higher strength than glass sheets [16]. This result proves that the presence of cracks and flaws in the material negatively affects its strength.

The theory behind stress concentration at crack tips stems from Griffith [14] and Irwin [17]. In a flaw-containing material subjected to a tensile stress, σ_∞, the stress in the vicinity of the crack tip, σ_c, is in fact much higher and decreases with increasing distance from the crack, as illustrated in Figure 2-9. According to Griffith [14], in an ideal elliptical flaw, the stress at the tip essentially depends on the flaw size and its sharpness, i.e. the radius of the crack opening:

$$\sigma_c = \sigma_\infty \left(1 + 2\sqrt{\frac{a}{\rho}}\right), \tag{2.8}$$

where a is the crack depth and ρ is the tip radius.

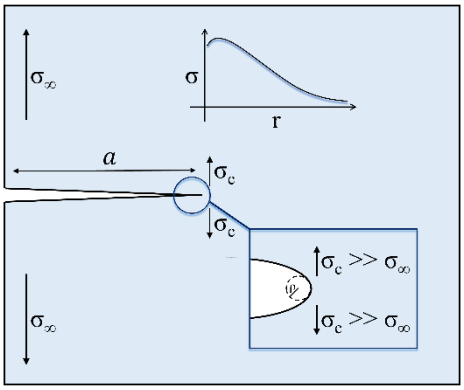

Figure 2-9 Schematic illustration of the stress concentration around the crack tip in a brittle material. The stress concentrates in the vicinity of the crack tip, and decreases with increasing distance from the tip. The stress at the crack tip, σ_c, is much larger than the far-field "infinite" stress, σ_∞.

The extent of stress concentration is expressed by the stress intensity factor, K, introduced by Irwin [17]. In a "type I" crack opening mode (i.e. with tensile stresses oriented normal on the crack), the stress intensity factor, K_I, depends on the far-field stress, σ_∞, and the depth of the flaw, a:

$$K_I = Y\sigma_\infty\sqrt{a}, \tag{2.9}$$

where Y is a geometric factor depending on the particular geometry of the specimen. The equation shows that increasing the stress or the flaw size results in an increase in K_I. Above a critical value of stress intensity, the crack is destined to propagate spontaneously, as the stress at crack tip overcomes the energy barrier governed by the intrinsic strength of the material. This value of K_I corresponds to the critical stress intensity factor, K_{Ic}, which is usually called the fracture toughness. In other words, fracture toughness describes how easy it is to break a specimen with a certain preexisting flaw.

The concept of fracture toughness becomes of practical use, because it is impossible to manufacture flawless test specimens of brittle materials, and the evaluation of the intrinsic strength is therefore extremely difficult. Knowing that cracks do not grow below K_{Ic}, but grow spontaneously above this value of stress intensity, K_{Ic} be

calculated from destructive experiments (usually pre-cracked beam bending) either by considering the work spent on breaking a given surface (Eq. 2.10), or by considering the peak load at fracture of a specimen with a known crack depth (Eq. 2.11):

$$K_{Ic} = \sqrt{\frac{2\gamma E}{1-\nu^2}}, \tag{2.10}$$

$$K_{Ic} = \frac{P}{B_{sp}\sqrt{W_{sp}}} Y_C^*, \tag{2.11}$$

where γ is the fracture surface energy (calculated from work of fracture and the corresponding surface area), E and ν are the Young's modulus and Poisson's ratio respectively, P is the peak load during fracture, B_{sp} and W_{sp} are the width and height of the specimen respectively, and Y_C is a factor depending on the geometry of the specimen and the depth of the crack.

K_{Ic} values of brittle materials are usually significantly lower than those of ductile materials, because the extent of plastic deformation in the former is limited [18]. In ductile materials, plasticity is easily initiated resulting in extensive crack tip blunting. As a consequence, the radius of the crack opening becomes larger, and the tensile stresses acting on the crack tip are more easily distributed. Hence, a much larger load is necessary to achieve spontaneous crack growth in a ductile material, leading to much higher critical stress intensity factors.

In order to determine K_{Ic}, one needs to perform a specimen failure test with a controlled flaw, from which the critical fracture must initiate. There are many available methods to probe K_{Ic}, e.g. single-edge-precracked beam (SEPB), chevron notch beam (CVB), single-edge notch beam (SENB), double cleavage drilled compression (DCDC), etc. [19]. These methods have different advantages as well as drawbacks. The SEPB method is the one preferred in this work due to the relative ease of inducing a sharp pre-crack necessary for a valid K_{Ic} determination in oxide glass.

In order to produce an SEPB specimen, a rectangular specimen is first polished to an optical finish. Then, a line of Vickers indents is made across the width of the specimen. Next, the specimen is subjected to bridge compression to allow the residual tensile stresses surrounding the Vickers indents to develop into a crack. This crack does not propagate throughout the specimen, but becomes arrested at certain point, when it reaches material under compression [20]. Finally, the pre-cracked specimen is subjected to three-point bending in order to fracture the beam. The peak load and the depth of the pre-crack (evaluated *post mortem*, see Figure 2-10) can be used to compute K_{Ic}, as described in section 2.2. Alternatively the work of fracture (i.e., the integrated area under a stable load-displacement curve) and the fracture surface area may be used to calculate the fracture surface energy, γ. This value can then be used to calculate K_{Ic} presuming the knowledge of Young's modulus, E, and Poisson's ratio, ν, of the glass. See detailed description of this method in Paper VII.

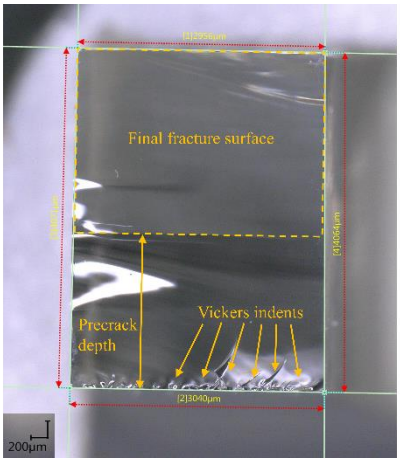

Figure 2-10 Optical micrograph of cross-section of a fractured SEPB specimen. The micrograph clearly illustrates a) the placement of Vickers indents, which are used to induce a precrack thanks to the residual tensile stress; b) the precrack developed through bridge compression; and c) the fracture surface resulting from three-point bending of the SEPB specimen. The illustrated SEPB is a specimen cut from a sodium aluminoborosilicate glass. Test details can be found in Paper VII.

2.4. SUMMARY

From a material design point of view, it is important to consider both the resistance to cracking induced by contact loading and the fracture toughness. A glass with a high damage resistance, but low toughness, is not very appealing, as some critical load will eventually lead to crack formation on the surface, putting the specimen at risk of failure upon additional strain. On the other hand, a glass with high toughness, but low resistance to contact loading, is also undesirable, since continuous damage of the surface will lead to a large flaw population, which in turn increases the probability of material breakage. In conclusion, a glass formulation exhibiting both high toughness and high crack resistance must be the target of the industry.

The resistance to indentation cracking strongly varies across different oxide glass compositions. In addition to that, any post-treatment method such as ion exchange or rapid cooling, as well as testing conditions strongly influence the extent of indentation cracking. On the other hand, fracture toughness does not vary significantly among different oxide glass formulations, but it is somewhat sensitive to the chemical composition. As mentioned in the previous chapter, the focus of this thesis lies on the link between the chemical composition and the fracture-related properties. However, to understand this link, one needs to have some insight into the arrangement of the atoms that constitute the glassy network, and how changes in the chemical composition of a given glass affect the structure of its network. This is the topic of the next chapter.

CHAPTER 3. FUNDAMENTALS OF OXIDE GLASS STRUCTURE

Glasses are amorphous, i.e. lacking the atomic periodicity known from crystals. This complicates the research in any field of glass science that relies on understanding of their structure, as there is no single structural unit that describes the entirety of the material. However, the arrangement of the atoms is not completely random. There is some degree of order on the short and to some extent the medium range. This chapter provides a fundamental description of how oxide glasses are arranged on the atomic scale, and how this affects material properties.

3.1. ATOMIC ARRANGEMENT IN GLASS

Oxide glasses are mixtures of any metal or half-metal oxides. Traditionally, they are synthesized by melting the oxide mixture at high temperature, and rapidly cooling the liquid into the glassy state. During cooling, a random three-dimensional network built of interconnected oxygen anions and metal or half-metal cations is formed. Each oxygen anion is linked to two cations, while each cation can link to a finite number of oxygen anions depending on its chemical properties. Such configuration of atoms, also called the random network, was originally suggested by Zachariasen [21], and later confirmed experimentally [22, 23]. However, because the bond angle distribution is larger than in their crystalline counterparts, there is no long range order [24], as illustrated in Figure 3-1.

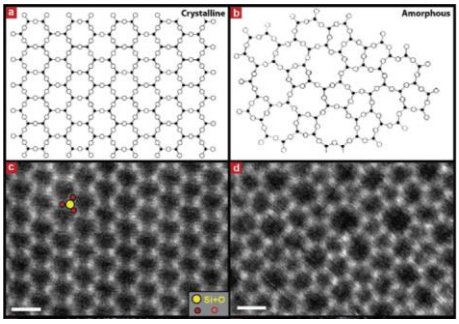

Figure 3-1 Annular dark-field scanning transmission electron microscopy images of crystalline (left) and amorphous (right) silica. The images were acquired on two-dimensional silica structures supported on graphene. The crystalline silica structures appears much more ordered compared to the amorphous network. The images are compared to schematic representations of structural configurations. Figure reprinted from Huang et al. [22] *with permission of American Chemical Society.*

The amount of oxygen anions surrounding a given cation (i.e., the coordination number) as well as the bond energy between the given anion-cation pair essentially depends on the size and valence of the cation of interest [25]. In other words, the position of a given element in the periodic table roughly dictates its chemical environment in the glass network. Based on this, different oxides can be grouped into:

- network formers (e.g. SiO_2 and B_2O_3), which form strongly bonded units with a low coordination number; these oxides constitute the backbone of the glassy network;
- network modifiers (e.g. Na_2O or CaO), which form units exhibiting high coordination numbers with ionic bonds; these oxides tend to depolymerize the glassy network;
- and intermediates (e.g. Al_2O_3), which can act as either of the two aforementioned categories depending on the remaining chemical composition of the glass.

This classification has been introduced for purely practical reasons, to facilitate the ease of discussing general trends in composition-structure-property relations. A few examples of how atoms are connected to each other in some common glassy networks, specifically aluminoborates and aluminosilicates which have been the main focus of this work, are provided in the next section.

3.2. SILICATE NETWORKS

The most simple and presumably most studied glass network is amorphous silica. Silica glass consists solely of tetrahedral units with a Si-atom in the center bonded to four O-atoms [26, 27]. Each O-atom acts as a bridge between two Si-atoms. For this reason, the O-atoms are referred to as bridging oxygens (BOs), while the building units are denoted as Q^4. The building units are thus the same as in crystalline silica, but due to a broader distribution of the bond angles between the Q^4 units, the structure becomes disordered, which is represented in Figure 3-2.

Upon addition of a modifying oxide, such as Na_2O, to amorphous silica, a richer structure emerges [28, 29]. Each pair of Na-cations has the ability to break up a Q_4-Q_4 link, resulting in two building units consisting of a Si-atom bonded to three BOs and one O-atom forming an ionic bond with a Na-cation. Such O-atom is called a non-bridging oxygen (NBO), since it no longer connects two adjacent Si-atoms, while the new building unit is denoted as Q_3. This can also be described as chemical reaction:

$$Si - O - Si + Na_2O \rightarrow Si - O^-Na^+ + Si - O^-Na^+. \quad (3.1)$$

Increasing the ratio between the modifying oxide and silica results in further depolymerization of the network, manifesting itself in creation of building units with

only two, one, and zero BOs, i.e., Q_2, Q_1, and Q_0 units, respectively [29]. The depolymerization of amorphous silica is illustrated in Figure 3-2.

The role of certain intermediate oxides, such as Al_2O_3, is also important to stress. The Al-cations tend to enter glassy networks including silicate-based ones in a fourfold coordination with O-atoms [30]. Given the position of Al in the periodic table, it is easy to derive the fact that the tetrahedral Al-unit carries a single negative charge. This configuration is stabilized if modifying cations, e.g. Na, are available in the glassy network. In that case, the positively charged Na-cations can balance the charge of the Al-units. Consequently, addition of Al_2O_3 to an alkali silicate glass results in a consumption of Na-NBO pairs, and repolymerizes the network. This is illustrated in Figure 3-2 as well.

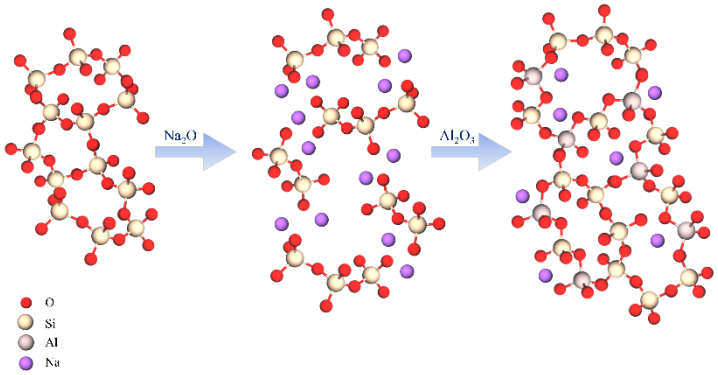

Figure 3-2 Representative sketch of atomic arrangement in silicate networks. Amorphous silica (left) consists of tetrahedral units (Q^4) with four bridging oxygens (BOs). Addition of a modifying oxide, e.g. Na_2O, leads to conversion of Q^4 units to Q^3 units (center), which are tetrahedral silicon atoms coordinated to three BOs and one non-bridging oxygen (NBO), Further addition would lead to formation of Q^2, Q^1, and eventually Q^0 species, with two, one, and zero BOs, respectively. Finally, addition of Al_2O_3 leads to consumption of NBOs (right), as tetrahedral aluminum units, Al^{IV},require charge-stabilization by Na-cations.

3.3. BORATE NETWORKS

The structure of borate glass, another important base network, differs from that of amorphous silica. Borate glass consists of trigonal units (B^{III}) encompassing a central B-atom bonded with three BOs [26, 31]. The first difference is thus apparent from the dimensionality of the network, where silica exhibits a highly cross-linked network. In addition, a relatively high degree of medium range order can be detected in borate glass, as the trigonal boron units form six-membered rings consisting of three B-atoms and three O-atoms, called boroxol rings [31, 32]. The structure of borate glass is illustrated in Figure 3-3.

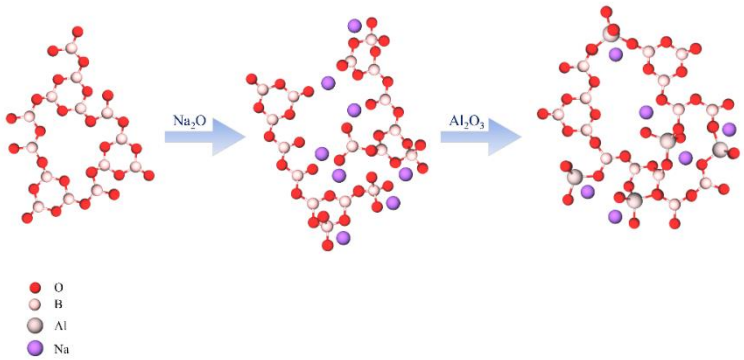

Figure 3-3 Representative sketch of atomic arrangement in borate networks. Vitreous boric oxide (left) consists solely of three-coordinated boron units, B^{III}. Addition of a modifying oxide, e.g. Na_2O, leads to conversion of B^{III} to tetrahedral units, B^{IV}, and formation of non-bridging oxygen atoms, NBOs (center). Both B^{IV} and NBOs are charge-stabilized by Na-cations. Finally, addition of Al_2O_3 leads to consumption of NBOs and B^{IV} (right), as tetrahedral aluminum units, Al^{IV}, compete for the Na-cations.

Upon addition of a modifying oxide to borate glass, another difference becomes apparent. Instead of depolymerizing the network through formation of NBOs, initial addition of a modifying oxide results in a conversion of trigonal boron units to tetrahedral ones [32, 33]. The position of B in the periodic table implies that a tetrahedral B-unit (B^{IV}) must carry a single negative charge, which can be balanced by an alkali or an alkaline earth metal cation, analogously to Al-tetrahedra. This essentially leads to an increase in the dimensionality of the borate network. However, it is important to note that at certain critical content of the modifying oxide, the structure cannot form more tetrahedral units, and depolymerized trigonal units with NBOs are formed instead [32, 33], similarly to the situation found in silica glass. This process is illustrated in Figure 3-3.

Addition of Al_2O_3 to an alkali borate has a similar impact as in silicate networks [34]. The Al-cations have a high affinity for the modifying metal cations, and thus tend to enter borate networks in tetrahedral configuration as well (Figure 3-3). In aluminoborate glasses, there is thus a competition for the modifying metal cations between B- and Al-atoms, usually shifted in favor of the Al-atoms [34, 35], as evident from the nuclear magnetic resonance spectra acquired on ^{11}B and ^{27}Al nuclei (Figure 3-4).

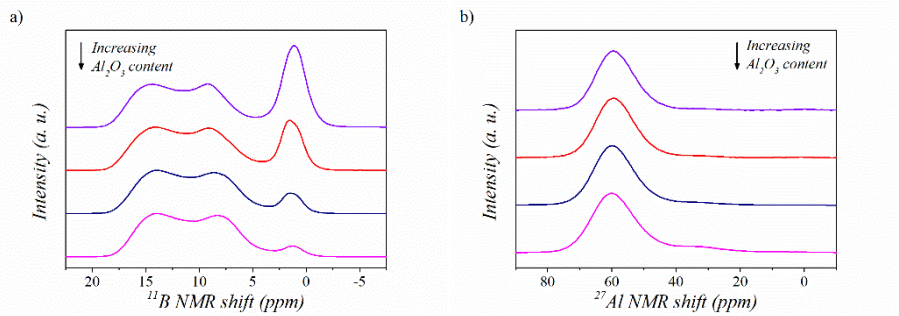

Figure 3-4 Solid state NMR spectra acquired on a series of sodium aluminoborate glasses with varying Al_2O_3/B_2O_3 content. a) ^{11}B MAS NMR spectra reveal that the fraction of tetrahedral boron, B^{IV}, decreases with increasing degree of Al_2O_3/B_2O_3 substitution. b) ^{27}Al MAS NMR spectra show less variation with most of aluminium in tetrahedral configuration, Al^{IV}. Figure adapted from Januchta et al. [36].

Finally, it is important to stress that the distribution of different building units in oxide glasses depends not only on the chemical composition, but also on the pressure and thermal history of the glass [37, 38]. This aspect is important when considering fracture and deformation characteristics of glasses, which are linked to the structural details of the glassy networks.

3.4. STRUCTURE-PROPERTY RELATIONS

The amount of bonds per atom as well as their strength obviously have an impact on material properties, as stronger bonds must logically improve the resistance to deformation, while higher amount of bonds make the material more rigid. In addition, the packing density of atoms also affects the material characteristics. These statements have shown to be true by collecting data for numerous chemical compositions.

One classical example of how structure affects the characteristics of the material is the prediction of glass transition temperature based on the topological constraint theory [39]. By employing the Phillips-Thorpe approach [40], wherein interatomic bonds are treated as constraints, and assigning a temperature dependence to those constraints, it is possible to construct a physical model capable of predicting viscosity of a given glass, and thereby its glass transition temperature. In such models, knowledge of the glassy network topology is crucial, as the amount of bonds per atom determines the amount of constraints, and thus the level of rigidity for a given glass composition at given temperature. This shows that structural details are essential for the purpose of material property prediction.

The topological approach has also been used to predict mechanical properties of oxide glasses, such as hardness and elastic moduli [41, 42]. In general, glasses with many bonds per atom are considered rigid, and display high resistance to structural

deformation, manifesting itself in high values of hardness and moduli. In the past, more simple models based on the dissociation energy of bonds and the bond density were suggested to predict hardness and elastic moduli as well [43, 44]. In these models, high average of bond strengths and high bond density have positive effect on the resistance to deformation, which agrees well with the fact that glasses consisting of strong bonds and highly connected glasses display high hardness and elastic moduli. The bond energy and density approach has also been used to predict fracture toughness in oxide glasses [18], although this is to the author's knowledge the only structure-based model for prediction of fracture-related properties. Also in this model, high density of bonds and their strength improves the resistance to crack growth, i.e., fracture toughness. In general, modelling of mechanical properties of glasses possess great potential with respect to design of new chemical compositions, but it continues to have some shortcomings and require further development.

3.5. SUMMARY

Although structure of oxide glasses is disordered, it can be described e.g. by the abundance of certain structural units. This structure can be easily influenced by adjusting the chemical composition, as both network formers, intermediates and modifiers have an impact on the connectivity of the network. The topology or the network structure has in turn an impact on the material properties of a given glass. In general, highly cross-linked glasses tend to strongly resist deformation, as their structural backbones are very rigid. On the other hand, glasses with relatively low dimensionality remain flexible and exhibit lower mechanical properties. These general rules should be treated with caution when designing new glass formulations, but can be applied to a certain extent of reliability. However, it is important to stress that the fracture-related properties, specifically the resistance to indentation cracking, are not merely depending on the structure of the pristine glass. In fact, it is also crucial to consider the structural changes undergoing during densification.

CHAPTER 4. DEFORMATION-STRUCTURE RELATIONS

Understanding the deformation mechanism of glasses subjected to contact loading appears to be the key to link the structural information with the tendency to initiate cracks. In order to reach to a better understanding of this aspect, researchers continuously study the mechanics of deformation on a continuity scale as well as the underlying changes occurring on the atomic scale of the glass during indentation. This chapter will highlight the core of the scientific findings related to indentation-induced deformation contributed by the author of this thesis.

4.1. DEFORMATION-INDUCED STRUCTURAL CHANGES

The chemical composition of a given glass dictates the deformation behavior of the material through its structure, as seen in Section 2.1. However, not only does the structure influence the deformation mechanism – the deformation also affects the structure. Micro-Raman spectroscopy may be used to probe such deformation-induced change to the glassy network. By focusing the laser beam inside a residual indentation imprint and comparing the spectrum with one acquired on pristine surface of the glass, it is possible to extract information with respect to the structural changes invoked in the material by indentation. This technique has been suggested in Ref. [45] and used to understand the nature of structural rearrangements occurring as a result of densification [46, 47]. An example of a structural change induced by indentation is given in Figure 4-1, where a La_2O_3-Al_2O_3-B_2O_3 (Paper IV) glass has been probed.

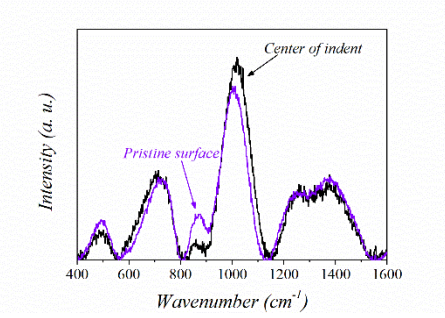

Figure 4-1 Raman spectra acquired in pristine surface (violet) and in the center of a Vickers indent (black) produced in a lanthanum aluminoborate glass. The figure represents an example of structural modification induced by indentation. Figure adapted from Paper IV.

The lanthanum aluminoborate glass subjected to indentation clearly undergoes changes in its networks structure, which is evident from the decrease in relative

intensity of the 850 cm^{-1} band and the increase in the 1000 cm^{-1} band. Such change could be associated with consumption of NBOs on pyroborate units and formation of B^{IV} units in diborate species (Paper IV). Several researchers have also employed Raman spectroscopy to determine the shape of the deformation zone and the extent of densification by comparing the spectra acquired within the indentation imprint to ones acquired in permanently compressed bulk glasses [48–50]. However, one needs to treat such data with caution, as it is practically impossible to control the volume of material subjected to laser irradiation, leading to potentially erroneous conclusions. Hence, it is advisable that Raman spectroscopy is to be used as a qualitative probe of structural rearrangements.

While the lanthanum aluminoborate glass exemplified above is a relatively complex structure, a few general structural changes occurring in oxide glasses are presented in the following. Amorphous silica is frequently studied with respect to densification, given the relatively good understanding of its structure and properties. The structural rearrangements induced by indentation of amorphous silica include the decrease of the $Si - O - Si$ tetrahedral angle within amorphous silica, as well as increasing abundance of three- and four-membered rings [46]. These observations, inferred from Raman spectroscopy, are in agreement with the higher density obtained through indentation. For modified silicate glasses, an increase in Q^2 abundance at the expense of Q^3 is recorded [51, 52]. In other words, a larger fraction of depolymerized tetrahedral units can be found in the structure of a deformed glass, suggesting extensive bond breakage. This finding could be linked to shear flow deformation, which is more pronounced in modified silicate glasses compared to amorphous silica [4]. The addition of repolymerizing oxides to modified silicate glasses, such as Al_2O_3 or B_2O_3, results in similar structural rearrangements to those recorded in amorphous silica [47]. This underlines the fact that connectivity plays an important role in the deformation mechanism of the glass.

In SiO_2-free borate networks, indentation results in reduction in distances between borate rings, broadening the $B - O - B$ bond angle distributions, and changing the abundance of different borate rings found in modified borate glasses [53]. In addition, a possible structural rearrangement involving conversion of B^{III} units to B^{IV} units has been suggested in this work (Paper I), as illustrated in Figure 4-2. Especially the latter mechanism may be used to explain the high propensity of borate glasses to densify. In other words, transition to a more closely packed local structure facilitates macroscopic densification.

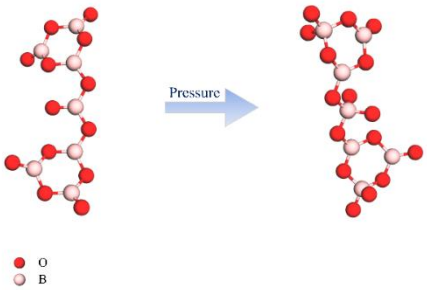

Figure 4-2 Representative sketch of a borate network subjected to pressure. B^{III} units convert to B^{IV} facilitating macroscopic densification.

In conclusion, deformation of oxide glasses can generally be associated with changes in bond lengths and bond angles, coordination numbers, and intermediate range order rearrangements.

4.2. STRUCTURE INFLUENCE ON DEFORMATION

Empirical work in the past has led to the conclusion that the extent of densification, quantified by V_R scales with the Poisson's ratio, v [4]. Poisson's ratio defines a material's response to elastic contraction or expansion in transverse direction upon loading in longitudinal direction. However, it is also suggested to be a metric of the network dimensionality in glasses [54], which merits the proposed correlation with V_R. However, reviewing the available data shows that the correlation is rather week (Paper V), as illustrated in Figure 4-3.

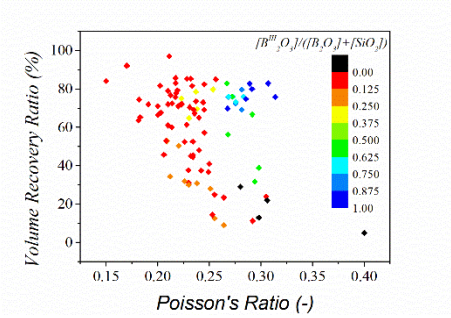

Figure 4-3 Volume recovery ratio as a function of Poisson's ratio. The majority of the data is for borate, silicate or borosilicate glasses (see Paper V). The data is indexed according to the fraction of B^{III} units relative to the total content of B_2O_3 and SiO_2, exposing an underlying dependence of V_R on chemical environment of the network. Black data points refer to glasses containing neither B_2O_3 nor SiO_2. Figure adapted from Paper V.

The figure shows that knowledge of v is not sufficient to predict the relative tendency of a glass to densify. A detailed inspection of the chemical compositions of glasses corresponding to the data points in Figure 4-3 have shown that some part of the scatter can be assigned to the network connectivity. Glasses rich in B^{III} tend to exhibit higher V_R values at given v values, insinuating that this structural unit facilitates densification, especially compared to the rigid tetrahedral B^{IV} units and Si^{IV} units (or mixed intermediate structures such as danburite rings [55]) abundant in the remainder of the examined data. This shows that the chemical composition has a large influence on the network structure, which in turn governs the deformation characteristics.

The reason behind the relatively high V_R values displayed by the B^{III}-rich glasses is the underlying atomic rearrangement induced by compressive stress. The difference between B^{III}–rich and B^{IV}–rich glasses is that in the latter, atoms are more efficiently packed in a three-dimensional network, while in the former, planar rings of atoms propagate through the structure. In other words, glasses abundant in B^{IV} units occupy less volume. Another important fact to point out is the reasonable stability of both B^{III} and B^{IV} units. As described in section 3.2, both species are frequently found in oxide glasses, and the distribution between them depends on several parameters, including chemical composition and processing conditions. This is in contrast to e.g. tetrahedral building blocks of silicate glasses, wherein Si-atoms occur almost exclusively in fourfold coordination with O-atoms. This translates into the tetrahedral configuration being much more thermodynamically favorable compared to e.g. six-coordinated Si-atoms, whereas the energetic difference between B^{III} and B^{IV} units is presumably relatively small. This allows local structures in B^{III}-rich glasses subjected to a compressive stress to "escape" into the B^{IV}-configuration, which is slightly less stable, but occupies less volume (Figure 4-2). This mechanism has been suggested as the driving force for densification in a crack-resistant lithium aluminoborate glass, reported in Paper I.

The positive effect of the possible B^{III} to B^{IV} conversion on densification is exemplified in the comparison of deformation characteristics of La_2O_3- and Al_2O_3-containing silicate, germanate, and borate glasses (Paper IV). The two former glasses exhibit strongly polymerized networks consisting of tetrahedral building blocks (germanate glasses are often analogous to silicates). On the other hand, the borate glass contains some fraction of B^{III}-units. Despite the three glasses having roughly the same Poisson's ratio, the borate glass exhibits almost double V_R value (Paper IV). This underlines the importance of considering the topology of the glass.

Within limited systems, where a given component is substituted systematically, logical correlations between the extent of densification and the chemical compositions may be found. One such example is the correlation between atomic packing density and L_{SR} (i.e., side length recovery acquired by optical microscopy measurements, see Section 2.1) in lanthanum zinc borate glasses (Paper VI). This shows that when the predominant structural rearrangement mechanism is the same in the glasses in

question, the free volume within the glassy network plays the governing role (Figure 4-4).

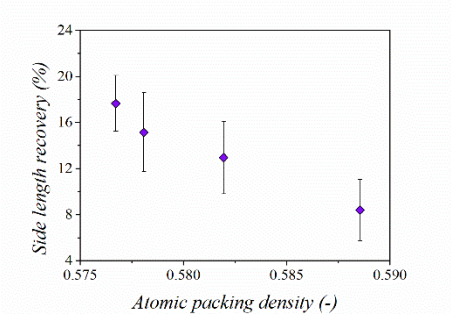

Figure 4-4 Side length recovery ratio as a function of atomic packing density for lanthanum zinc borate glasses. The scatter plot shows that within an isolated system, where the substitution of constituents is relatively small, a good agreement between the extent of densification and network packing can be observed. Figure computed from data presented in Paper VI.

In the above, it was illustrated that the nature of the network-forming oxide cation, specifically its ability to attain different configurations, plays a significant role in the deformation mechanism. However, this work also found that the network-modifying oxide cation affects the densification potential (Paper II). By substituting the alkali oxide in an aluminoborate base glass, V_R changes significantly, as illustrated in Figure 4-5, where the increasing field strength of the alkali cation (i.e., charge to radius squared ratio) leads to a decrease in V_R. Further substitution to MgO (Paper III), an alkaline earth oxide, confirms this trend.

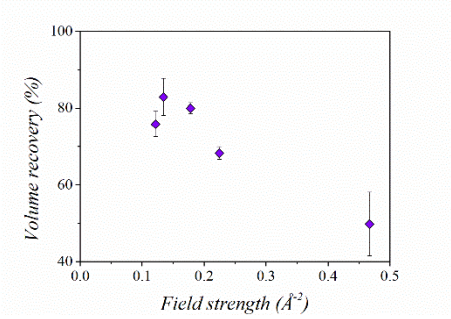

Figure 4-5 Volume recovery ratio as a function of modifying cation field strength for a series of aluminoborate glass at fixed Al_2O_3/B_2O_3 ratio. The scatter plots illustrates that the network-modifying oxide may strongly influence the deformation mechanism. Figure adapted from Paper II with addition of data from magnesium aluminoborate glass (Paper III). Note that the low field strength data point corresponds to the rubidium glass, which may exhibit self-recovery of the indent cavity, similarly to the ceasium aluminoborate glass (see Paper VIII).

4.3. SUMMARY

The indentation deformation mechanism governs the extent of stress dissipation and thus the tendency to crack initiation. Hence, studying the deformation-induced structural changes is very important. In this work it was shown that knowledge of possible structural rearrangements in a given glass unmasks its potential to densify, and thus facilitates design of compositions with a certain tendency to adapt to stress. In general, borate glasses, specifically ones rich in trigonal boron units such as aluminoborates, tend to exhibit higher extents of densification then more rigid silicate glasses. The conversion of trigonal intro tetrahedral boron has been suggested as the main mechanism responsible for this difference. However, other oxide components and structural characteristics such as atomic packing density have been shown to affect the deformation mechanism within isolated systems.

CHAPTER 5. COMPOSITION-FRACTURE RELATIONS

The ability to accurately predict material properties based on the chemical composition is the ultimate goal of any material design specialist. In oxide glasses, understanding of the composition and properties are linked through the structure of the glass network. Hence, it is of interest to report any findings related to the structure-property correlations. In this chapter, the findings related to how structure, and in part chemical composition, affect the fracture-related properties will be presented.

5.1. CRACK RESISTANCE

Mechanical properties of oxide glasses such as elastic moduli and hardness can be predicted to a certain degree [41, 43, 44]. Theoretically, it should also be possible to predict *CR* for a given chemical composition based on the insight into its network structure. The most frequent approach to solve this problem is the use of the extent of indentation-induced densification, which is said to quantify the potential to dissipate work during loading. Metrics of the densification extent can be V_R or L_{SR}, as mentioned in Section 2.1. However, the correlations between *CR* and V_R (Paper I) as well as *CR* and L_{SR} (Paper IX) are poor (Figure 5-1). The former correlation is drawn for different oxide glass systems, where the data has been compiled from various research facilities, while the latter correlation depicts a single sodium aluminoborosilicate glass system synthesized and characterized by the author. In either case, there is an overall positive trend between *CR* and the given recovery ratio, but the data scatter is significant.

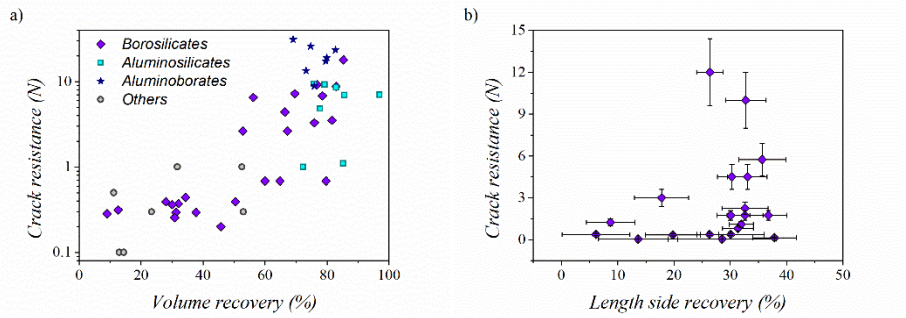

Figure 5-1 a) Correlation between crack resistance and volume recovery ratio for various oxide glass systems. Figure adapted from Paper I. b) Correlation between crack resistance and length side recovery ratio for a specific sodium aluminoborosilicate system. Figure adapted from Paper IX. Both scatter plots show that while there is a general positive correlation between the extent of densification and resistance to crack initiation, the scatter in data is relatively large.

The trends illustrated in Figure 5-1 prove that it is currently too challenging to design glass compositions with a specific target value of *CR*. Nevertheless, researchers are now aware of certain structural features, which facilitate densification, and thus improve *CR*. An example of such structure-based control of *CR* is the inclusion of trigonal boron units, B^{III}. These species tend to convert to tetrahedral B^{IV} units when subjected to a compressive stress, as to minimize the local volume around the unit, as described in section 4.2. In this work, it was shown that the abundance of such structural rearrangements could be a factor governing the tendency to initiate cracks (Paper I). In order to access this information, several glasses were isostatically compressed at high temperature, and their pristine and compressed states were analyzed in terms of coordination numbers of the network-forming nuclei using solid-state NMR. The gain in average coordination number and the extent of densification, normalized to the applied pressure, were then used to compute a value describing the ease of a given glassy network to adapt to compressive stress, i.e., the *atomic self-adaptivity* defined in Paper I as:

$$Atomic\ self adaptivity = \langle \Delta n \rangle \frac{\Delta \rho}{\rho_0 P}, \tag{5.1}$$

where $\langle \Delta n \rangle$ is the pressure-induced change in average coordination number of network-forming cations (Si, B, or Al) as determined by NMR, $\Delta \rho$ is the change in bulk density of the glass, ρ_0 is the initial density, and P is the applied isostatic pressure. A reasonable correlation between *CR* and the atomic self-adaptivity (Figure 5-2) suggests that the connectivity of the material and especially the potential of change in connectivity have a strong influence on *CR*. It is noteworthy that aluminosilicate glasses appear to deviate slightly from the trend, suggesting that some structural rearrangements (e.g. change in silicate ring structures) not captured by the model (only accounting for changes in coordination numbers) may be facilitating densification.

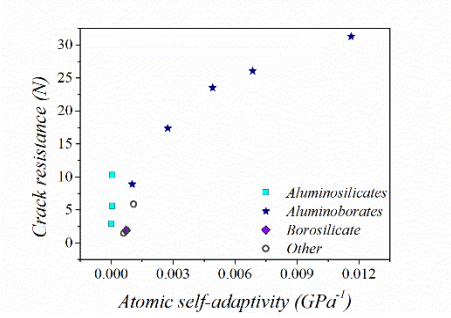

Figure 5-2 Correlation between crack resistance and atomic self-adaptivity. The scatter plot suggests that resistance to indentation cracking is governed by the extent of structural rearrangements in the glassy network, which facilitate macroscopic densification. Data points correspond to aluminosilicate, aluminoborate, borosilicate, and boroaluminophosphosilicate glasses. Figure adapted from Paper I.

It is noteworthy that the extent of densification is not necessarily governed by the abundance of B^{III} units, but rather by the potential of those units to convert into B^{IV}. In other words, a given B^{III}-rich glass may not densify very well, if its structure lacks the ability to stabilize the B^{IV} units in the compressed state. Indeed, the sodium aluminoborate glasses shown in Figure 5-2 contain more B^{III} [36] than the lithium aluminoborate glass.

Unfortunately, the access to local shifts in connectivity limited to the vicinity of the indentation site remains challenging, and even the plot illustrated above is merely an approximation with certain assumptions. Consequently, more feasible predictors of *CR* related to the structural details of glasses are necessary in order to facilitate efficient glass composition design. By reviewing the available *CR* data, a correlation with a product of V_R and the average dissociation energy of the oxide bonds, E_D, constituting the corresponding glassy network was suggested (Paper V), yielding a positive correlation (Figure 5-3). The plot is a representation of different oxide glass systems, and gathers all available V_R data. The E_D data were computed from Ref. [56]. It is important to stress that only data for oxide glasses evaluated in ambient humid atmosphere was used to compute the plot, since humidity may strongly affect the propensity to initiate cracks [57, 58]. This phenomenon will be discussed in detail in section 5.3.

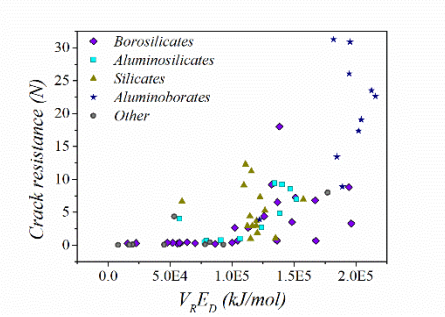

Figure 5-3 Crack resistance as a function of the product of volume recovery ratio, V_R, and average bond energy, E_D. The scatter plot illustrates that a glass needs to exhibit a combination of high strength and high ability to densify in order to be crack-resistant. The data points correspond to silicates, borosilicates, aluminobsilicates, aluminoborates and other networks. Figure adapted from Paper V.

The product of V_R and E_D has no physical meaning. However, it clearly illustrates that at least two different parameters have an influence on *CR*. The former, V_R, is a quantification of the relative extent of indentation-induced densification, as explained in Section 2.1. When the value is high, the glass undergoes extensive densification, which consumes significant amount of work supplied to the glass during indentation, and therefore the residual stresses which act as a driving force for the crack initiation are small. The latter, E_D, describes the necessary energy to break an oxide bond in the network. Hence, networks consisting of strong bonds, i.e. large E_D values, must

exhibit large resistances against crack opening through systematic cleavage of those bonds. It is therefore evident that in order to achieve a high *CR*, the glass needs to exhibit high ability to dissipate the supplied work (i.e., high V_R) and high resistance towards bond breakage driven by the non-dissipated work (i.e., high E_D).

5.2. FRACTURE TOUGHNESS

The notion that brittleness in glasses is controlled by the chemical energy stored in their networks has previously been suggested by Rouxel [18]. In this case, the dissociation energy of bonds involved in fracture was used to predict the fracture surface energy, and by extension fracture toughness, K_{Ic}. This work investigated the applicability of the suggested model on the prediction of SEPB-measured K_{Ic} values for a range of sodium aluminoborosilicate glasses (Paper VII). The agreement between the modelled and the empirically acquired toughness values is poor (Figure 5-4).

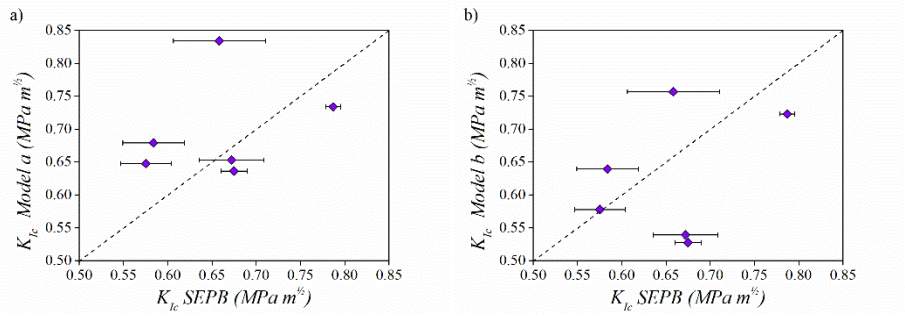

Figure 5-4 Correlation between empirical fracture toughness values and modelled values as described in Paper VII. In model a), it is assumed that one bond per cation is broken. In model b), it is assumed that exactly half of the B^{III} units remain intact. The scatter plots thus illustrate the importance of considering the actual path of the propagating crack when predicting fracture toughness. Figures computed from data available in Paper VII.

The lack of a one-to-one agreement was suggested to be related to the network connectivity. The modelled values presented in Figure 5-4 take into account an average of all oxide bonds found in the network. However, it is possible that the crack front avoids cleavage of certain bonds, if a more energetically favorable path is available. Such situation is theoretically possible since glasses consist of a mixture of weak bonds to modifying cations and strong bonds between an oxygen anion and a network forming cation, while the coordination numbers are fluctuating throughout the network (Figure 5-5). Taking into account the possibility to avoid certain structural units, e.g. B^{III}-containing rings, which are only connected to the network along two dimensions, the modelled K_{Ic} values may decrease in several cases. This underlines the necessity to access information regarding the actual crack path in order to enable proper understanding of crack growth in oxide glasses.

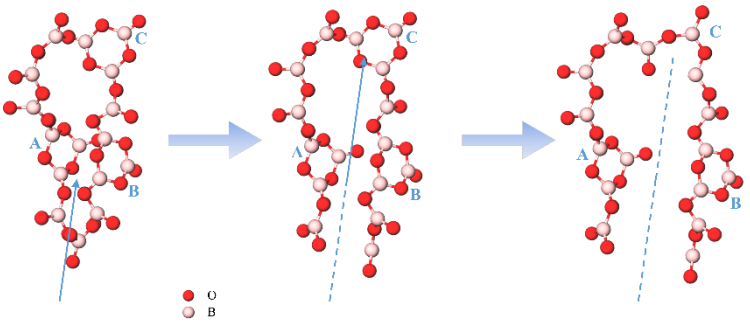

Figure 5-5 Sketch of a borate network subjected to breakage. In this scenario, boroxol rings A and B are aligned parallel to the propagating crack front, and avoid bond cleavage. Boroxol ring C is positioned perpendicular to the crack front and is therefore subject to a B–O bond cleavage. The illustration demonstrates that crack front may avoid certain structural units and still propagate through the network. Such situation has a negative influence on fracture toughness, as less bonds need to be cleaved in order to propagate a given unit of distance.

The dissociation energy of the oxide bonds determine the energy input to allow a growing crack to surpass a pair of atoms, and it was shown to be an important parameter both for *CR* and for K_{Ic}. This would suggest that there may be a correlation between these two metrics of glass brittleness. However, for the relatively small dataset encompassing both *CR* and K_{Ic} available for oxide glasses, there appears to be no correlation. For the investigated sodium aluminoborosilicate glasses (Papers VII and IX), the points are significantly scattered (Figure 5-6).

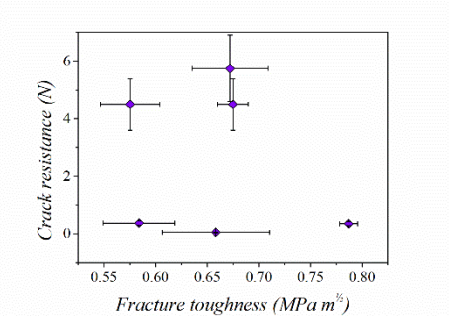

Figure 5-6 Crack resistance as a function of fracture toughness measured using the SEPB technique for sodium aluminoborosilicate glasses. The scatter plot reveals the lack of correlation between the two quantities. Figure adapted from Paper IX.

There is a reason behind the lack of correlation, although both properties describe the brittle behavior of a glass. Despite the fact that E_D has a positive influence on the resistance to crack initiation and crack growth, it is not the most crucial parameter. Instead, the impact of the network connectivity on the crack extension, crack

initiation, as well as the preceding deformation mechanism, should be considered. Rigid glasses with fully polymerized network are expected to exhibit high resistances to crack growth, as the crack front has a limited possibility to avoid any structural units. However, those fully polymerized networks tend to resist densification, as the potential to induce volume-decreasing structural rearrangements is low, which in turn leads to storage of large residual stresses and hence results in low *CR*. On the other hand, flexible networks with a low dimensionality can easily densify, but they may experience that the crack front navigates through the easily broken domains of the material. In conclusion, the network connectivity may have opposite effects on *CR* and K_{Ic}, respectively, which explains the lack of correlation between them.

5.3. EFFECT OF HUMIDITY

The characteristics of crack initiation and growth in oxide glasses are known to be influenced by the level of humidity. In general, water molecules in the atmosphere are believed to hydrolyze the oxide bonds in glass [59], especially when they are stressed, according to the following reaction:

$$Si - O - Si + H_2O \rightarrow Si - OH + Si - OH. \tag{5.2}$$

The result of this chemical process is essentially formation of two new surfaces, since the network is no longer polymerized by the oxide bond. This process continues stepwise as new bonds become hydrolyzed, corresponding to a growing crack.

However, there are also examples of water having a positive influence on the crack-related properties in oxide glasses. Hydrothermally treated glasses exhibit higher *CR* and strength compared to their pristine states [60, 61]. This phenomenon was also observed in this work.

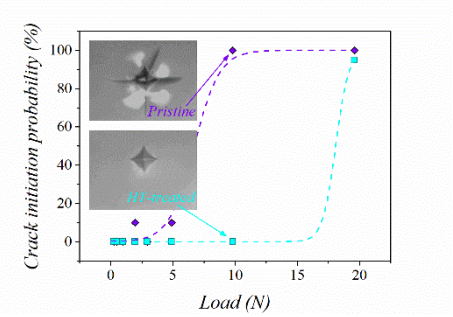

Figure 5-7 Crack initiation probability as a function of load for a sodium magnesium boroaluminosilicate glass. The pristine glass (top inset) exhibits 100 % probability of corner cracking at 9.81 N load, in contrast to the hydrothermally-treated (HT) glass (bottom inset), which exhibits no cracks at this load. Crack resistance increases from ~7 N to ~15 N due to the hydrothermal treatment.

A sodium magnesium boroaluminosilicate glass was subjected to an 18 h cycle in an autoclave at 140 °C and 368 kPa of water vapor pressure. Then, the *CR* values of the pristine and the hydrothermally treated glass were determined (see details in Figure 5-7).

Another example of water strengthening is presented in Paper VIII. The investigated caesium aluminoborate glass appears to reach record-high values of *CR*, which is exemplified by the 490 N crack-free Vickers indent (Figure 5-8).

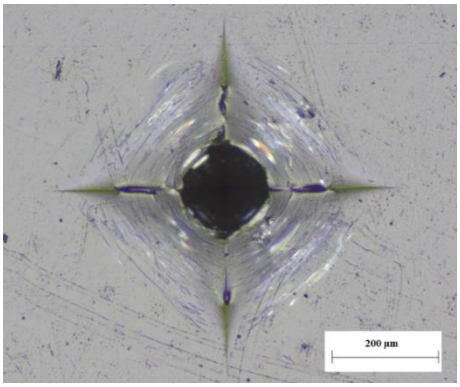

Figure 5-8 Optical microscopy image of a 490N Vickers indent produced in aged ceasium aluminoborate glass. The indent does not exhibit any corner cracks. Image reprinted from Paper VIII under the Creative Commons BY 4.0 license.

It appears that producing crack-free indents at such high magnitudes of load is only possible when the pristine glass has been exposed to humid atmosphere for an extended amount of time. The indent impression illustrated in Figure 5-8 has been aged for 7 days in ambient conditions (room tempetarure, ~40 % RH). In addition, the indent site appears to shrink over time of exposure to humid environment. The mechanism governing the increase in *CR* as well the swelling behavior was suggested in this work (Paper VIII). As illustrated in Figure 5-9, atmospheric water is believed to diffuse into the hygroscopic glass network, which results in expansion of the material leading to formation of a compressive zone at the surface inhibiting crack initiation. Alternatively, the water depolymerizes the network, which results in a more flexible material being able to more easily accommodate the work supplied during indentation.

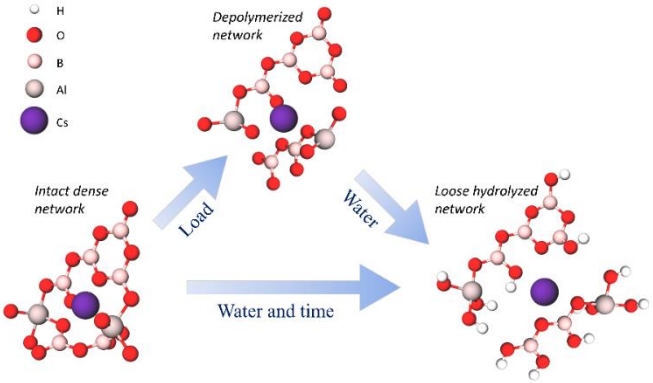

Figure 5-9 Sketch of the deformation and hydration mechanism induced by indentation of the ceasium aluminoborate glass. The structure suffers from bond breakage, which exposes sites that are easily hydrolyzed by water molecules diffusing into the glass. This forces the network to expand in order to accommodate the water, either physically or chemically bound. Figure reprinted from Paper VIII under the Creative Commons BY 4.0 license.

By extension, the author suggests that the same or a similar mechanism is responsible for the increase in *CR* of the hydrothermally treated glasses (Figure 5-7). The reason why this increase is not recorded by exposure to ambient conditions is the high chemical durability of the investigated glass, which can be overcome by increasing the water activity level, e.g. by application of a vigorous treatment such as hydrothermal aging. Future work should address this proposed explanation.

5.4. SUMMARY

Fracture toughness can to some extent be predicted based on the knowledge of the chemical composition of the glass. However, further research is necessary to shed light on the characteristics of crack front propagation. This work pointed to certain aspects, which can be addressed, specifically the possibility to avoid certain structural units depending on the connectivity of the glass. Addressing this will hopefully improve the predictive potential of the current model.

Crack resistance is a more complicated measure of brittleness, as it is influenced by several parameters. It has been shown that high tendency to densify promotes the resistance to crack initiation. As does high strength of bonds constituting the network. Finally, atmospheric conditions can have a positive or negative influence on the value of crack resistance. In conclusion, design of crack-resistant glasses is currently very challenging, since e.g. improving the bond strength could lead to a decrease in densification potential. Future work, based on the findings provided in this work, will possibly make the material design process more efficient.

CHAPTER 6. PERSPECTIVES

Throughout the thesis, examples of the impact of the chemical composition and network structure of oxide glasses on their deformation and cracking characteristics have been presented. In this chapter, the main findings will be briefly summarized along with a discussion concerning their significance and suggestions regarding future work.

Oxide glasses display a densification behavior when subjected to sharp-contact loading, but the relative extent of densification strongly varies among the known chemical compositions. The literature consensus used to be that the propensity to densify depends on the atomic packing density of the glass or on its Poisson's ratio. This is only true to some extent, as a very large spread in the data arises when examining a wide range of glasses. The variations are due to the differences in the connectivity of the atomic network, with glasses exhibiting low dimensionality being able to densify more compared to rigid strongly polymerized glasses. This finding shows that it is practically impossible to design a new glass composition with a certain target value of the extent of densification, but on the other hand, it underlines the structural features, which promote the densification on atomic scale. One can thus incorporate or remove such structural motifs in order to tune the deformation mechanism.

The tendency to initiate cracks following impact by a sharp object is herein investigated in terms of indentation experiments. It is well acknowledged that the propensity to densify results in stress dissipation, or in other words, in a smaller driving force for indentation cracking. Although a general positive correlation between the relative densification extent and crack resistance, *CR*, is apparent from the available data, structural details of the glasses result in data scattering. It is shown that not only the tendency to densify, but also the structural features facilitating that densification, govern the tendency to initiate cracks following indentation. In addition, it is suggested that *CR* is a product of two parameters: on one hand, the extent of densification, which is inversely correlated with the potential to initiate cracks; on the other, the bond strength, which is positively correlated with the resistance to crack extension. These findings prove that design of more crack-resistant glasses requires strong oxide components, which also facilitate stress-induced atomic-scale rearrangements.

The crack growth resistance, characterized by fracture toughness, K_{Ic}, has been shown to scale well with the strength of the bonds found in a given glass. In this work, some discrepancy between an existing model and empirical toughness values has been discovered. The conclusions drawn from this study is that the propagating crack may choose the thermodynamically favorable path. In other words, the strong bonds in a given chemical composition may not necessarily be involved in the fracture process,

provided that some degree of heterogeneity exists in the glass. This underlines that while there is a big predictive potential in the existing K_{Ic} model, sophisticated knowledge regarding the local structure fracture process is required as input into the model. This will surely be addressed by future studies.

In extension of the K_{Ic} studies, it is noticed that the connectivity of the glass may have opposite effects on K_{Ic} and on *CR* (through densification potential). At the same time, bond strength is believed to have a positive effect on both metrics. This creates significant scatter when comparing K_{Ic} and *CR* data, leading to the conclusion that there is no correlation between these two properties. The significance of this discovery is twofold: (i) any assumptions regarding crack-resistant glass being tough or vice versa should be avoided, as K_{Ic} and *CR* are fundamentally different measures of glass brittleness; (ii) future material design targeted at commercial applications would in most cases need to address both properties.

Finally, the impact of water on the strength of glasses is usually assumed to be negative. This continues to be the case with regard to numerous aspects. However, this work has shown that positive development in fracture-related properties, specifically *CR*, can be achieved by allowing the glass to interact with atmospheric humidity. This has led to the suggestion of a molecular-scale mechanism, which accounts for the humidity-induced increase in *CR* as well as a swelling behavior recorded for a certain glass composition. Several other mentions of positive influence of water on cracking in glasses have been reported in the literature, proving that the presented glass is not a unique exception from the rule. In author's opinion, this finding poses a motivation for future studies regarding the chemical interaction between water and oxide glass networks. Hopefully, the improved understanding of how water influences the fracture and deformation characteristics from a structural point of view will facilitate the possibility to develop new materials with improved mechanical properties.

BIBLIOGRAPHY

1. Fischer-Cripps AC (2007) Introduction to contact mechanics, 2nd ed. Springer Science

2. Marsh DM (1964) Plastic Flow in Glass. Proc R Soc A Math Phys Eng Sci 279:420–435

3. Peter KW (1970) Densification and flow phenomena of glass in indentation experiments. J Non Cryst Solids 5:103–115

4. Yoshida S, Sangleboeuf J-C, Rouxel T (2005) Quantitative evaluation of indentation-induced densification in glass. J Mater Res 20:3404–3412

5. Rouxel T (2015) Driving force for indentation cracking in glass: composition, pressure and temperature dependence. Philos Trans A Math Phys Eng Sci. doi: 10.1098/rsta.2014.0140

6. Lawn BR, Swain M V. (1975) Microfracture beneath point indentations in brittle solids. J Mater Sci 10:113–122

7. Arora A, Marshall DB, Lawn BR, Swain M V. (1979) Indentation deformation/fracture of normal and anomalous glasses. J Non Cryst Solids 31:415–428

8. Kato Y, Yamazaki H, Yoshida S, Matsuoka J (2010) Effect of densification on crack initiation under Vickers indentation test. J Non Cryst Solids 356:1768–1773

9. Striepe S, Deubener J, Potuzak M, Smedskjaer MM, Matthias A (2016) Thermal history dependence of indentation induced densification in an aluminosilicate glass. J Non Cryst Solids 445–446:34–39

10. Johnson KL (1970) The correlation of indentation experiments. J Mech Phys Solids 18:115–126

11. Yoffe EH (1982) Elastic stress fields caused by indenting brittle materials. Philos Mag A 46:617–628

12. Sellappan P, Rouxel T, Celarie F, Becker E, Houizot P, Conradt R (2013) Composition dependence of indentation deformation and indentation cracking in glass. Acta Mater 61:5949–5965

13. Wada M, Furukawa H, Fujita K (1974) Crack Resistance of Glass on Vickers Indentation. In: Proc. Xth Int. Congr. Glas. p 39

14. Griffith AA (1921) The Phenomena of Rupture and Flow in Solids. Philos Trans R Soc London Ser A, Contain Pap a Math or Phys Character 221:163–198

15. Varshneya AK (2018) Stronger glass products: Lessons learned and yet to be learned. Int J Appl Glas Sci 9:140–155

16. Mould RE (1967) The Strength of Inorganic Glasses. In: Fract. Met. Polym. Glas. Springer US, Boston, MA, pp 119–149

17. Irwin GR, Kies JA, Smith HL (1958) Fracture strengths relative to onset and arrest of crack propagation. In: Proc. ASTM. pp 640–657

18. Rouxel T (2017) Fracture surface energy and toughness of inorganic glasses. Scr Mater 137:109–113

19. Rouxel T, Yoshida S (2017) The fracture toughness of inorganic glasses. J Am Ceram Soc 100:4374–4396

20. To T, Célarié F, Roux-Langlois C, Bazin A, Gueguen Y, Orain H, Le Fur M, Burgaud V, Rouxel T (2018) Fracture toughness, fracture energy and slow crack growth of glass as investigated by the Single-Edge Precracked Beam (SEPB) and Chevron-Notched Beam (CNB) methods. Acta Mater 146:1–11

21. Zachariasen WH (1932) The atomic arrangement in glass. J Am Chem Soc 54:3841–3851

22. Huang PY, Kurasch S, Srivastava A, et al (2012) Direct Imaging of a Two-Dimensional Silica Glass on Graphene. Nano Lett 12:1081–1086

23. Lichtenstein L, Büchner C, Yang B, Shaikhutdinov S, Heyde M, Sierka M, Włodarczyk R, Sauer J, Freund H-J (2012) The Atomic Structure of a Metal-Supported Vitreous Thin Silica Film. Angew Chemie Int Ed 51:404–407

24. Farnan I, Grandinetti PJ, Baltisberger JH, Stebbins JF, Werner U, Eastman MA, Pines A (1992) Quantification of the disorder in network-modified silicate glasses. Nature 358:31–35

25. Sun K-H (1947) Fundamental Condition of Glass Formation. J Am Ceram Soc 30:277–281

26. Warren BE, Krutter H, Morningstar O (1936) Fourier analysis of X-ray patterns of vitreous SiO2 and B2O2. J Am Ceram Soc 19:202–206

27. Brückner R (1970) Properties and structure of vitreous silica. I. J Non Cryst Solids 5:123–175

28. Greaves GN (1985) EXAFS and the structure of glass. J Non Cryst Solids 71:203–217

29. Maekawa H, Maekawa T, Kawamura K, Yokokawa T (1991) The structural groups of alkali silicate glasses determined from ^{29}Si MAS-NMR. J Non Cryst Solids 127:53–64

30. Seifert FA, Mysen BO, Virgo D (1982) Three-dimensional network structure of quenched melts (glass) in the systems SiO_2-$NaAlO_2$, SiO_2-$CaAl_2O_4$ and SiO_2-$MgAl_2O_4$. Am Mineral 67:696–717

31. Krogh-Moe J (1969) The structure of vitreous and liquid boron oxide. J Non Cryst Solids 1:269–284

32. Konijnendijk WL, Stevels JM (1975) The structure of borate glasses studied by Raman scattering. J Non Cryst Solids 18:307–331

33. Zhong J, Bray PJ (1989) Change in boron coordination in alkali borate glasses, and mixed alkali effects, as elucidated by NMR. J Non Cryst Solids 111:67–76

34. Gresch R, Müller-Warmuth W, Dutz H (1976) ^{11}B and ^{27}Al NMR studies of glasses in the system Na_2O-B_2O_3-Al_2O_3 (“NABAL”). J Non Cryst Solids 21:31–40

35. Züchner L, Chan JCC, Müller-Warmuth W, Hellmut E (1998) Short-Range Order and Site Connectivities in Sodium Aluminoborate Glasses: I. Quantification of Local Environments by High-Resolution 11B, 23Na, and 27Al Solid-State NMR. J Phys Chem B 102:4495–4506

36. Januchta K, Youngman RE, Goel A, Bauchy M, Rzoska SJ, Bockowski M, Smedskjaer MM (2017) Structural origin of high crack resistance in sodium aluminoborate glasses. J Non Cryst Solids 460:54–65

37. Stebbins JF, Ellsworth SE (1996) Temperature Effects on Structure and Dynamics in Borate and Borosilicate Liquids: High-Resolution and High-Temperature NMR Results. J Am Ceram Soc 79:2247–2256

38. Lee SK, Eng PJ, Mao H, Meng Y, Newville M, Hu MY, Shu J (2005) Probing of bonding changes in B_2O_3 glasses at high pressure with inelastic X-ray scattering. Nat Mater 4:851–854

39. Gupta PK, Mauro JC (2009) Composition dependence of glass transition temperature and fragility. I. A topological model incorporating temperature-dependent constraints. J Chem Phys 130:94503

40. Phillips JC, Thorpe MF (1985) Constraint theory, vector percolation and glass formation. Solid State Commun 53:699–702

41. Smedskjaer MM, Mauro JC, Yue Y (2010) Prediction of Glass Hardness Using Temperature-Dependent Constraint Theory. Phys Rev Lett 105:115503

42. Wilkinson CJ, Zheng Q, Huang L, Mauro JC (2019) Topological constraint model for the elasticity of glass-forming systems. J Non-Crystalline Solids X 2:100019

43. Makishima A, Mackenzie JD (1973) Direct calculation of Young's modulus of glass. J Non Cryst Solids 12:35–45

44. Yamane M, Mackenzie J. (1974) Vicker's Hardness of glass. J Non Cryst Solids 15:153–164

45. Kailer A, Nickel KG, Gogotsi YG (1999) Raman microspectroscopy of nanocrystalline and amorphous phases in hardness indentations. J Raman Spectrosc 30:939–946

46. Perriot A, Vandembroucq D, Barthel E, Martinez V, Grosvalet L, Martinet C, Champagnon B (2006) Raman Microspectroscopic Characterization of Amorphous Silica Plastic Behavior. J Am Ceram Soc 89:596–601

47. Winterstein-Beckmann A, Möncke D, Palles D, Kamitsos EI, Wondraczek L (2014) A Raman-spectroscopic study of indentation-induced structural changes in technical alkali-borosilicate glasses with varying silicate network connectivity. J Non Cryst Solids. doi: 10.1016/j.jnoncrysol.2014.09.020

48. Kassir-Bodon A, Deschamps T, Martinet C, Champagnon B, Teisseire J, Kermouche G (2012) Raman Mapping of the Indentation-Induced Densification of a Soda-Lime-Silicate Glass. Int J Appl Glas Sci 3:29–35

49. Kato Y, Yamazaki H, Yoshida S, Matsuoka J, Kanzaki M (2012) Measurements of density distribution around Vickers indentation on commercial aluminoborosilicate and soda-lime silicate glasses by using micro

Raman spectroscopy. J Non Cryst Solids 358:3473–3480

50. Deschamps T, Kassir-Bodon A, Sonneville C, Margueritat J, Martinet C, de Ligny D, Mermet A, Champagnon B (2013) Permanent densification of compressed silica glass: a Raman-density calibration curve. J Phys Condens Matter. doi: 10.1088/0953-8984/25/2/025402

51. Deschamps T, Martinet C, Bruneel JL, Champagnon B (2011) Soda-lime silicate glass under hydrostatic pressure and indentation: a micro-Raman study. J Phys Condens Matter 23:35402

52. Kato Y, Yamazaki H, Yoshida S, Matsuoka J, Kanzaki M (2012) Measurements of density distribution around Vickers indentation on commercial aluminoborosilicate and soda-lime silicate glasses by using micro Raman spectroscopy. J Non Cryst Solids. doi: 10.1016/j.jnoncrysol.2012.04.035

53. Yoshida S, Nishikubo Y, Konno A, Sugawara T, Miura Y, Matsuoka J (2012) Fracture- and Indentation-Induced Structural Changes of Sodium Borosilicate Glasses. Int J Appl Glas Sci 3:3–13

54. Rouxel T (2007) Elastic Properties and Short-to Medium-Range Order in Glasses. J Am Ceram Soc 90:3019–3039

55. Limbach R, Winterstein-Beckmann A, Dellith J, Möncke D, Wondraczek L (2015) Plasticity, crack initiation and defect resistance in alkali-borosilicate glasses: From normal to anomalous behavior. J Non Cryst Solids 417–418:15–27

56. Luo Y-R, Cheng J-P Handbook of Chemistry and Physics, 86th ed. Talor & Francis

57. Pönitzsch A, Nofz M, Wondraczek L, Deubener J (2016) Bulk elastic properties, hardness and fatigue of calcium aluminosilicate glasses in the intermediate-silica range. J Non Cryst Solids 434:1–12

58. Bechgaard TK, Mauro JC, Smedskjaer MM (2018) Time and humidity dependence of indentation cracking in aluminosilicate glasses. J Non Cryst Solids 491:64–70

59. Wiederhorn SM (1967) Influence of Water Vapor on Crack Propagation in Soda-Lime Glass. J Am Ceram Soc 50:407–414

60. Lezzi PJ, Xiao QR, Tomozawa M, Blanchet TA, Kurkjian CR (2013) Strength

increase of silica glass fibers by surface stress relaxation: A new mechanical strengthening method. J Non Cryst Solids 379:95–106

61. Luo J, Huynh H, Pantano CG, Kim SH (2016) Hydrothermal reactions of soda lime silica glass – Revealing subsurface damage and alteration of mechanical properties and chemical structure of glass surfaces. J Non Cryst Solids 452:93–101

LIST OF PUBLICATIONS

PUBLICATIONS IN PEER-REVIEWED JOURNALS

Contributed as first author or main co-author:

K. Januchta, R.E. Youngman, A. Goel, M. Bauchy, S.L. Logunov, S.J. Rzoska, M. Bockowski, L.R. Jensen, and M.M. Smedskjaer, "Discovery of ultra-crack-resistant oxide glasses with adaptive networks", *Chemistry of Materials*, **29** (2017) 5865-5876

K. Januchta, M. Bauchy, R.E. Youngman, S.J. Rzoska, M. Bockowski, and M.M. Smedskjaer, "Modifier field strength effects on densification behavior and mechanical properties of alkali aluminoborate glasses", *Physical Review Materials*, **1** (2017) 063603

K.F. Frederiksen, **K. Januchta**, N. Mascaraque, R.E. Youngman, M. Bauchy, S.J. Rzoska, M. Bockowski, and M.M. Smedskjaer, "Structural compromise between high hardness and crack resistance in aluminoborate glasses", *The Journal of Physical Chemistry B*, **122** (2018) 6287-6295

K. Januchta, R. Sun, L. Huang, M. Bockowski, S.J. Rzoska, L.R. Jensen, and M.M. Smedskjaer, "Deformation and cracking behavior of La_2O_3-doped oxide glasses with high Poisson's ratio", *Journal of Non-Crystalline Solids*, **494** (2018) 86-93

K. Januchta and M.M. Smedskjaer, "Indentation deformation in oxide glasses: Quantification, structural changes, and relation to cracking," *Journal of Non-Crystalline Solids X*, **1** (2019) 100007

K. Januchta, R.E. Youngman, L.R. Jensen, and M.M. Smedskjaer, "Mechanical property optimization of a zinc borate glass by lanthanum doping", *Journal of Non-Crystalline Solids*, **520** (2019) 119461

K. Januchta, T. To, M. Bødker, T. Rouxel, and M.M. Smedskjaer, "Elasticity, hardness, and fracture toughness of sodium aluminoborosilicate glasses", *Journal of American Ceramic Society*, **102** (2019) 4520-4537

K. Januchta, M. Stepniewska, L.R. Jensen, Y. Zhang, M.A.J. Somers, M. Bauchy, Y.Z. Yue, and M.M. Smedskjaer, "Breaking the limit of micro-ductility in oxide glasses", *Advanced Science*, (2019) 1901281

K. Januchta, P. Liu, S.R. Hansen, T. To, and M.M. Smedskjaer, "Indentation cracking and deformation mechanism of sodium aluminoborosilicate glasses", manuscript submitted to *Journal of American Ceramic Society*

Contributed as co-author:

S. Kapoor, **K. Januchta**, R.E. Youngman, X. Guo, J.C. Mauro, M. Bauchy, S.J. Rzoska, M. Bockowski, L.R. Jensen, M.M. Smedskjaer, "Combining high hardness and crack resistance in mixed network glasses through high-temperature densification", *Physical Review Materials*, **2** (2018) 063603

N. Mascaraque, K.F. Frederiksen, **K. Januchta**, R.E. Youngman, M. Bauchy, M.M. Smedskjaer, "Competitive effects of modifier charge and size on mechanical and chemical resistance of aluminoborate glasses", *Journal of Non-Crystalline Solids*, **499** (2018) 264-271

N. Mascaraque, **K. Januchta**, K.F. Frederiksen, R.E. Youngman, M. Bauchy, M.M. Smedskjaer, "Structural dependence of chemical durability in modified aluminoborate glasses", *Journal of American Ceramic Society*, **102** (2019) 1157-1168

M.B. Østergaard, S.R. Hansen, **K. Januchta**, T. To, S.J. Rzoska, M. Bockowski, M. Bauchy, M.M. Smedskjaer, "Revisiting the dependence of Poisson's ratio on liquid fragility and atomic packing density in oxide glasses", *Materials*, **12** (2019) 2439

P. Liu, **K. Januchta**, L.R. Jensen, M. Bauchy, M.M. Smedskjaer, "Competitive effects of free volume, rigidity, and self-adaptivity on indentation response of silicoaluminoborate glasses", *Journal of American Ceramic Society*, paper accepted, early view available (doi.org/10.1111/jace.16790)

M. Stepniewska, **K. Januchta**, C. Zhou, A. Qiao, M.M. Smedskjaer, Y.Z. Yue, "Anomalous cracking in a metal-organic framework glass", submitted manuscript, preprint available at ChemRxiv (doi.org/10.26434/chemrxiv.7844720.v1)

ORAL AND POSTER PRESENTATIONS AT CONFERENCES

K. Januchta, R.E. Youngman, A. Goel, M. Bauchy, S.J. Rzoska, M. Bockowski, M.M. Smedskjaer, "Correlating densification and crack resistance in sodium aluminoborate glasses", *7th International Workshop on Flow and Fracture of Advanced Glasses*, Aalborg, Denmark, 2017

K. Januchta, K.F. Frederiksen, M. Bauchy, R.E. Youngman, M.M. Smedskjaer, "Tuning mechanical properties of aluminoborate glasses by modifier substitution", *7th International Congress on Ceramics*, Iguacu Falls, Brazil, 2018

K. Januchta, T. To. T. Rouxel, M.M. Smedskjaer, "Fracture toughness and indentation cracking resistance in the Na_2O-Al_2O_3-B_2O_3-SiO_2 chemical system", *15th International Conference on Physics of Non-Crystalline Solids"*, Saint-Malo, France, 2018

K. Januchta, R. Sun, L. Huang, M.M. Smedskjaer, "Characterization of deformation and cracking behavior of high Poisson's ratio oxide glasses with La_2O_3", *15th International Conference on Physics of Non-Crystalline Solids"*, Saint-Malo, France, 2018

K. Januchta, M. Stepniewska, Y.Z. Yue, L.R. Jensen, Y. Zhang, S.S. Much, M.A.J. Somers, M.M. Smedskjaer, "Observation of Crack-Free Vickers Indents at 500 N in Annealed Caesium Aluminoborate Glass", *25th International Congress on Glass*, Boston, MA, United States, 2019

K. Januchta, T. To, T. Rouxel, M.M. Smedskjaer, "Deformation and fracture behavior of Na2O-Al2O3-B2O3-SiO2 glasses", *25th International Congress on Glass*, Boston, MA, United States, 2019

ISSN (online): 2446-1636
ISBN (online): 978-87-7210-509-3

AALBORG UNIVERSITY PRESS